



**University  
of Basel**

Department of  
Biomedical Engineering



**Politecnico  
di Torino**

Niccoló Porciani

# **Design, Implementation, and Evaluation of a Sterile Workflow for Robot-Assisted Laser Ablation of Cartilage Tissue**

**Master Thesis**

**Supervision**

Cédric Duverney

**Advisor**

Prof. Dr. Georg Rauter  
Prof. Dr. Enrica Verné  
Prof. Dr. Andrea Barbero

October 2023



# Abstract

The ability to spontaneously heal articular cartilage injuries is extremely limited. This aspect is even more evident in full-thickness lesions. Healthy knee joint chondrocytes are difficult to harvest without further damage to the articular surface. The autologous grafts based on them have shown many drawbacks after being implanted. The researchers of the Department of Biomedicine at the University of Basel are currently developing an innovative kind of autologous graft, using nasal chondrocytes as a more appropriate source of cells. However, for the transplant to be successful, the dimension and the shape of the graft must fit the articular defect. Previous studies have demonstrated how refreshing cartilage defects or reshaping the graft using surgical tools might be highly harmful, reducing the probability of success of the implant. On the other hand, promising results have been noted when these procedures are performed through laser ablation. Further investigation is required to better understand the actual benefits of using lasers in place of standard tools. However, working with biological tissue requires a lot of precautions to keep the samples sterile and alive during the cutting process. Hence, the aim of this work was to develop a container that allows to perform laser-based experiments without contamination or damage to biological samples. The design must guarantee flexibility during the experiments and the possibility of using the container in any environment, even in unsterile ones. The core of the following pages is the description of the adopted workflow, from the analysis of the issues of the previous container to the manufacturing of the new one. Among them, are the phases of designing, prototyping and updating the list of requirements. The final device is a compact, autoclavable and biocompatible box that is suitable to be used in different experimental setups involving sterile samples. The 3 DoF inner platform and the movable laser transparent sapphire window enable the user to focus the laser light on different parts of the sample, with the possibility to change its inclination and distance from the laser source. Besides, custom-made airtight junctions are meant to ensure sterility during the experiments. It could be demonstrated through laser ablation experiments on human cartilage samples that the proposed device complies with all fundamental requirements. Thus, this device can in the future be used to further investigate laser-cartilage interactions first in an ex vivo laboratory setting, and eventually in vivo trials.

# Acknowledgements

This section is dedicated to all the people who have supported and helped me over the last five years. First of all I want to thank my family, it is thanks to them that I learned what it means to commit to achieving your goals. Thanks also to my grandparents, to those who are still with us and to those who support me from up there. I could never forget my lifelong friends, thank you Scazzon Boys for always being there to cheer me up, even in the happiest and saddest moments. Thanks also to my friends from Turin, even if we have only known each other for two years, I am sure that our bond will last a long time. Finally, I want to thank my colleagues at Biomed-Lab who have welcomed me and made me feel part of their team over the last six months.



---

# Declaration of Originality

I hereby declare that the written work I have submitted entitled

**Design, Implementation, and Evaluation of a Sterile Workflow for Robot-Assisted Laser Ablation of Cartilage Tissue**

is original work which I alone have authored and which is written in my own words<sup>1</sup>

## Author(s)

Niccoló Porciani

## Supervision

Cédric Duverney

With the signature I declare that I have been informed regarding normal academic citation rules. The citation conventions usual to the discipline in question here have been respected.

The above written work may be tested electronically for plagiarism.

Basel, 6/10/2023  
Place and date

  
Signature

---

<sup>1</sup>Co-authored work: The signatures of all authors are required. Each signature attests to the originality of the entire piece of written work in its final form.

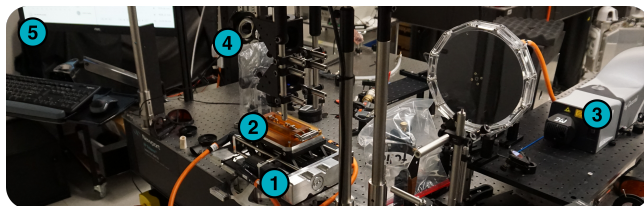




## Master Thesis: Design, Implementation, and Evaluation of a Sterile Workflow for Robot-Assisted Laser Ablation of Cartilage Tissue

**Context:** Cartilage damage in the knee joint can be caused by aging or repetitive actions. It can be treated by surgically removing the damaged cartilage tissue and filling the generated defect with a precisely shaped, healthy cartilage graft [1]. Nowadays, removing the defected cartilage is done manually using surgical curettes or scalpels. This approach is simple and quick, but only provides limited cutting accuracy. Moreover, removing defected cartilage exactly down to subchondral bone is not possible by hand. However, regenerative grafts will only reintegrate and survive if placed in the correct layer without leaving defective cartilage behind. Thus, we are developing a system (a) leveraging robotic positioning and laser light for precise, controlled, and contactless tissue ablation [2, 3].

**Task description:** A workflow and container (b) for sterile laser ablation of tissue has been designed and validated [2]. However, several limitations related to sample handling and fixation, ease of use, and robustness have been identified in the current design. Your task will be to design and manufacture a new sterile ablation container addressing these issues, to adapt the overall sterile ablation workflow towards higher intuitiveness and usability especially for novice users, and to validate your design in a sterile laser ablation experiment.



(a) The developed tissue preparation system with (1) robotic stage, (2) biological sample, (3) ablation laser, (4) camera, and (5) graphical user interface.



(b) A cartilage sample fixed in the current sterile ablation container.

### Work packages:

- Review the relevant literature on sterile laser ablation of soft tissue.
- Detail requirements for sterile workflow and container based on application and insights from past experiments.
- Define an optimized sterile ablation workflow.
- Design and manufacture your new sterile ablation container.
- Perform laser ablation of live cartilage tissue with your workflow and validate process sterility.

### Benefits:

- Gain practical experience with mechanical design for biomedical applications.
- Learn to work with lasers for biological tissue ablation.
- Apply sterility tests and gain experience with interpreting their results.
- Work in a highly interdisciplinary team of robot engineers, laser physicists, and biologists.

### Requirements:

- Solid background in biomedical or mechanical engineering or a closely related field.
- Basic knowledge of mechanics, materials, and physics.
- Prior experience with mechanical design is a plus, but not strictly required.

### References:

- [1] M. Mumme et al. "Nasal chondrocyte-based engineered autologous cartilage tissue for repair of articular cartilage defects: an observational first-in-human trial." *The Lancet*, 388(10055), pp. 1985-1994, Oct. 2016. doi.org/10.1016/S0140-6736(16)31658-0
- [2] C. Duverney et al. "Sterile Tissue Ablation Using Laser Light - System Design, Experimental Validation, and Outlook on Clinical Applicability." *J. Med. Devices*, 15(1), pp. 11104/1-11104/12, Mar. 2021. doi.org/10.1115/1.4049396
- [3] L. Beltrán Bernal et al. "Laser in Bone Surgery." In: S. Stübinger et al. (eds), *Lasers in Oral and Maxillofacial Surgery*, pp. 99-109, Springer, Cham, Mar. 2020. doi.org/10.1007/978-3-030-29604-9\_9

Student: Niccolò Porciani  
Start: April 2023  
Duration: 6 months

biomed.dbc.unibas.ch  
blog.dbc.unibas.ch  
biomedizin.unibas.ch/barbero-lab

### Supervision:

Cédric Duverney (cedric.duverney@unibas.ch)  
Dr. Ferda Canbaz

### Professors:

Prof. Dr. Georg Rauter  
Prof. Dr. Andrea Barbero

# Symbols

## Symbols

## Acronyms and Abbreviations

MIRACLE	Minimally Invasive Robot-Assisted Computer-guided Laserosteotome
BIROMED	Bio-inspired Robots for Medicine Lab
BLOG	Biomedical Laser and Optics Group
LAROCARE	Laser-assisted Robot-guided Cartilage Regeneration
DBE	Department of Biomedical Engineering
DBM	Department of Biomedicine
Nd:YAG Laser	Neodymium-Doped Yttrium Aluminium Garnet Laser
Er:YAG Laser	Erbium-Doped Yttrium Aluminium Garnet Laser
MMP-13	Matrix Metalloproteinase-13
OCT	Optical Coherence Tomography

# Contents

<b>Abstract</b>	i
<b>Acknowledgements</b>	ii
<b>Declaration of Originality</b>	iii
<b>Task Description</b>	iv
<b>Symbols</b>	vi
<b>1 Introduction</b>	<b>2</b>
1.1 LAROCARE project . . . . .	2
1.2 Current state of the project . . . . .	3
1.3 Motivations and goals . . . . .	3
<b>2 Literature review</b>	<b>4</b>
2.1 Osteoarthritis . . . . .	4
2.2 Drawbacks of current techniques for cartilage repair . . . . .	4
2.3 New kind of grafts . . . . .	4
2.4 Laser ablation . . . . .	5
2.5 Laser ablation of cartilage tissue . . . . .	6
<b>3 Methods</b>	<b>7</b>
3.1 Requirements . . . . .	7
3.1.1 Meeting with DBM biologists . . . . .	7
3.1.2 Meeting with BLOG laser physicists . . . . .	10
3.2 First list of requirements . . . . .	11
3.3 Old container . . . . .	13
3.3.1 Components . . . . .	14
3.3.2 Pros and cons . . . . .	15
3.4 Design process . . . . .	18
3.5 First prototype . . . . .	19
3.5.1 Designing and prototyping . . . . .	19
3.5.2 Pros and cons . . . . .	22
3.6 Second list of requirements . . . . .	25
3.7 Second prototype . . . . .	27
3.7.1 Designing and prototyping . . . . .	27
3.7.2 Pros and cons . . . . .	31
3.8 Third list of requirements . . . . .	34
3.9 Third prototype . . . . .	35
3.9.1 Designing and prototyping . . . . .	35
3.9.2 Pros and cons . . . . .	38
3.10 Manufacturing . . . . .	41

---

<b>4</b>	<b>Testing</b>	<b>46</b>
4.1	Sealing tests . . . . .	46
4.1.1	Water-tightness test . . . . .	46
4.1.2	Air-tightness test . . . . .	47
4.2	Usability test . . . . .	49
4.3	Autoclave test . . . . .	50
4.4	Laser setup fitting test . . . . .	51
<b>5</b>	<b>Conclusion</b>	<b>53</b>
5.1	Summary . . . . .	53
5.2	Conclusion . . . . .	55
5.3	Future work . . . . .	56

# List of Figures

2.1	Laser-tissue interaction map depending on power density and exposure time <a href="#">[1]</a> . . . . .	5
2.2	Cell viability after laser and surgical scissors reshape in surrounding tissues 0-200 $\mu m$ (black bars) and 200-400 $\mu m$ (grey bars) distant from the cutting edge at different times <a href="#">[2]</a> . . . . .	6
3.1	Anatomy of the knee joint. The femoral condyles are the two rounded prominences at the end of the femur, the tibial plateau is the flat top portion of the tibial bone. . . . .	7
3.2	Picture of the entire knee joint sample harvested during surgery. . . . .	8
3.3	Picture of the tibial plateau extracted from the whole sample. . . . .	8
3.4	Resizing of the tibial plateau to fit inside the new container. The procedure was performed by Prof. Barbero using surgical pliers and shears. . . . .	9
3.5	Picture of the final sample obtained using surgical tools. . . . .	9
3.6	Picture of the Nd:YAG pulsed laser. . . . .	10
3.7	Picture of the Er:YAG pulsed laser. . . . .	10
3.8	Picture of the old container, completely assembled. The total height is about 26 cm and the diameter of the bottle is approximately 10 cm. . . . .	13
3.9	Pictures from two different points of view of the sapphire lid, the diameter of the sapphire window is around 5 cm. . . . .	14
3.10	Picture of the glass bottle. . . . .	14
3.11	Pictures from two different points of view of the sample holder. . . . .	14
3.12	This plot gives the measured total transmission of the 5 mm thick sapphire window. . . . .	15
3.13	Debris expulsion during laser ablation in three different moments. . . . .	16
3.14	The picture shows the flowchart followed during the design process. . . . .	18
3.15	The picture shows the CAD project of the first prototype. . . . .	19
3.16	Picture of the laser cutter Glowforge Plus. . . . .	20
3.17	Picture of the 3D printer Fortus 250mc. . . . .	20
3.18	The picture shows the prototype realized in acrylic and 3D printed material. The dimensions of the box are approximately 22x14x21 cm . . . . .	21
3.19	In the picture on the left it is possible to observe the black silicon ring used to seal the hole for the knob, in the picture on the right it is shown the orange ring that seals the attachment between the cage plate and the box. . . . .	22
3.20	Top view of the container, the red phantom in the center of the sapphire window represents the cartilage sample. . . . .	22
3.21	In the pictures it is shown the sample holder in two different configurations. The maximum achievable inclination in one direction is about $25^\circ$ , which means that the overall range of motion around the rotation axis is $50^\circ$ . . . . .	23
3.22	The figure shows the images from which the ML and the AP are measured, on the left the view from above of the tibial plateau generated through CT, on the right the frontal and lateral view of the knee joint obtained through CR <a href="#">[3]</a> . . . . .	25
3.23	The picture shows the second prototype. The dimensions of the box are approximately 14x13x18 cm and the reservoir has a volume of 0.4 l. . . . .	27
3.24	The picture shows the platform meant to hold the sample during the laser ablation. . . . .	28
3.25	On the left the rectangular slots on the sides of the base, on the right the spherical joint that couples the base and the sample holder. . . . .	28

3.26	The picture shows the first stage of the mechanism and a simplified version of the platform on which the sample will be placed. . . . .	29
3.27	On the left, the actuation of the platform along the x-axis. On the right, the actuation of the platform is along the y-axis. . . . .	29
3.28	The picture shows how the second stage works if the gear g3 is coupled to the gear g1.	30
3.29	Three different possible spatial orientations achievable through the described stage. . . . .	30
3.30	In the picture the two possible configurations: when the reservoir is above the level of the fluid in the box, the fluid flows towards the box and vice versa when it is under. . . . .	31
3.31	The picture shows the distance between the platform and the sapphire glass. The minimum safety distance to avoid debris deposit is about 5 cm. . . . .	32
3.32	The picture shows the second prototype completely disassembled. . . . .	32
3.33	The picture shows the third prototype. The dimensions of the box are approximately 9x16x16 cm while the upper part has a diameter of 10 cm . . . . .	35
3.34	The picture shows the main box and the inner mechanism. . . . .	36
3.35	On the left the rotation around the x-axis, on the right the rotation around the y-axis.	36
3.36	On the left the two clamps are concentric, on the right they are displaced. . . . .	37
3.37	The pictures show how every extremity of the platform can be reached by the laser beam by moving the sapphire window relative to the container. . . . .	37
3.38	The clamps can be adjusted through the screw shown in the picture, ensuring a tight sealing between the membrane and the container. . . . .	38
3.39	The picture shows how the platform can be lifted up and down depending on whether the sample has to be ablated or kept safe and hydrated. . . . .	38
3.40	The picture shows the platform used in the third prototype. . . . .	39
3.41	The picture shows the final device, the dimensions of the lower box are 9x16x16 cm. . . . .	41
3.42	The picture shows the polycarbonate box before the manufacturing. . . . .	42
3.43	The picture shows the four holes drilled in the top side of the box. . . . .	42
3.44	The picture shows one of the three custom-made screws and the three nuts. The overall length of the leadscrew is 10 cm. . . . .	43
3.45	The picture shows how the mechanism appears when it is extracted from the box. . . . .	43
3.46	The picture shows the top and bottom sides of the aluminum knobs. . . . .	43
3.47	On the upper side of the transparent layer, the orange silicon ring. On the other side, the white Teflon ring. . . . .	44
3.48	The picture shows the bottom of the box and the Teflon component in white. . . . .	44
3.49	The picture shows the bottom of the box and the Teflon component in white. . . . .	45
4.1	Standard-case scenario: the device is filled with water and the height of the fluid is 3 cm, enough to cover completely the platform. . . . .	46
4.2	Worst-case scenario: the device is filled with water and the height of the fluid is 7 cm, enough to cover completely the seal. . . . .	47
4.3	On the left, the upper part of the seal as it was purchased. On the right, the same part after the insertion of the silicon layer . . . . .	47
4.4	On the left, one of the two seals for the membrane. On the right, the seal for the knobs.	48
4.5	The picture shows the silicon ring placed between the membrane and the clamp. . . . .	48
4.6	On the left, the applied weight to the membrane is 0.2 kg. On the right, it is 0.8 kg. . . . .	48
4.7	The pictures show the sample inside the old container in two possible configurations: submerged and above the level of the fluid. . . . .	49
4.8	The pictures show the sample inside the new container in two possible configurations: submerged and above the level of the fluid. . . . .	49
4.9	Pictures of the autoclave, model "Vertical 3870ELV". . . . .	50
4.10	Experimental setup. . . . .	51
4.11	On the left, the attachment between the cage plate and optic system. On the right, the 2 DoF stage is placed under the container. . . . .	52
4.12	The green point shows where the laser beam would perform the ablation. . . . .	52
5.1	A picture from the usability test. . . . .	53
5.2	Workflow, from the harvesting of the sample to the post-experiment analysis [4]. . . . .	55



# List of Tables

3.1	Specifications of the two aforementioned lasers.	10
3.2	First list of requirements for the new container.	12
3.3	Requirements with which the old container complies (green) or does not comply (red) from the first list.	17
3.4	Requirements with which the first prototype complies (green) or does not comply (red) from the first list.	24
3.5	Second list of requirements, the requirements that have been changed compared to the first list are written in blue.	26
3.6	Requirements with which the second prototype complies (green) or does not comply (red) from the first list.	33
3.7	Third list of requirements, the requirements that have been changed compared to the second list are written in blue.	34
3.8	Requirements with which the third prototype complies (green) or does not comply (red) from the first list.	40
3.9	List of materials used to manufacture the final device.	45
4.1	Autoclave cycle.	51
5.1	Requirements with which the final device complies (green) or does not comply (red) from the third list.	54

# 1 Introduction

In the last few years, the enormous steps forward in the robotic and automation field have led to a larger use of automatic components in medical applications, to reach a much higher level of accuracy and safety. Although surgeons are extremely competent and experienced, cutting human tissues through surgical tools might be extremely harmful to the tissue itself and affect the viability of the cells, furthermore, the perfect repeatability of the procedure cannot be assured.

Within the MIRACLE project [5], the BIROMED-Lab (Bio-Inspired RObots for MEDicine-Laboratory) together with the BLOG (Biomedical Laser and Optics Group) is currently trying to overcome the aforementioned limitations by developing new automated robotic devices, to provide reliable help during mini-invasive surgical operations. The group's main focus is to standardize the cutting of hard tissues and make it as repeatable as possible, reducing the impact on the tissue around the surgical site and the risk of infection. To achieve such high precision in minimally invasive procedures some specific subsystems are requested like stabilization mechanisms, flexible endoscopes and dedicated optics systems. However, the development of innovative medical devices must be supported by the design of an appropriate user-friendly graphic interface that eases the task of the surgeon and keeps the patient safe from eventual dangerous errors. The final aim of the project is to gather these different kinds of subsystems in just one multifunctional robotic platform, that could be able to perform high-precision cuts on various types of human tissues and become part of the operating room's ordinary instrumentation. Soon after the start of the project, the idea of developing a high-precision laser to ablate knee cartilage grafts arose, this device would allow not only to obtain more accurate and less hurtful cuts on the tissue but also to carry out this procedure directly in the surgery environment as a part of the described platform. So, in 2019 the LAROCARE project was founded to pursue this highly complex purpose.

## 1.1 LAROCARE project

One of the most challenging goals of today's medical research is finding a safe and standardized method to enhance the healing ability of the cartilage tissue of damaged human joints. The main worldwide cause of articular damage is osteoarthritis, it is estimated that over 50 million people suffer from this disease only in the USA and, at the same time, there is a large number of patients who are affected by invalidating joint injuries. Several techniques have been proposed during the last decades but no one of these seems to have sufficient requirements to become the "gold standard" in this field.

The LAROCARE (LAsEr-assisted ROBot-guided CARtilage REgeneration), born from the collaboration between the Departments of Biomedical Engineering (DBE) and of Biomedicine (DBM) at the University of Basel, is working on setting the standard in this field through a specific workflow for cartilage grafts, starting from the harvesting of human chondrocytes until the positioning in the knee. The procedure begins with the collection of autologous nasal chondrocytes that are used to produce custom grafts for the patient, then the defects in the cartilage are refreshed using a system leveraging robotic positioning and laser light for precise, controlled, and contactless tissue ablation. When the defects have the desired shape, the grafts can be easily sutured to the healthy knee cartilage reducing the risk of failure of the implant. In parallel to the aforementioned workflow, a suitable protocol must be implemented to keep the specimens alive and sterile during all the different operations, otherwise, the produced grafts would be completely unusable. As in other biomedical tasks, also this project needs the optimal balance between engineered technology and strict biological requirements.

## 1.2 Current state of the project

The overall work can be divided into three different subprojects which are being developed simultaneously to integrate them, once everyone is sufficiently ready:

- **Grafts manufacturing and positioning:** This is the section of the project carried on by Professor Andrea Barbero and his team at the DBM, their job starts with the harvesting of nasal chondrocytes and ends when the autologous cartilage grafts are ready to be implanted. In one of the latest related publications [6], the results of the first related human trial are described as strongly positive and promising for the future progress of the technique. Ten patients with full-thickness cartilage lesions on the femoral condyle or trochlea were treated, the engineered tissues were implanted into the defects and evaluated 24 months after surgery. No adverse reactions were observed and self-assessed clinical scores for pain, knee mobility, and quality of life were improved significantly.
- **Laser's parameters optimization and validation:** At the moment, Nd:YAG and Er:YAG lasers have been used on pathologic and live articular cartilage samples, with encouraging outcomes regarding cell viability in alive ones. However, laser parameters such as pulse frequency and energy need to be optimized toward higher cutting efficiency, all while ensuring that cells close to the cut are not being mechanically damaged or carbonized. In the future will be necessary to test different setups for various parameters, to validate them by ablating live cartilage samples and performing histological analyses to evaluate cell damage.
- **Sterile workflow implementation:** A workflow and a container for sterile laser ablation of tissue have been designed. Nevertheless, several limitations related to sample handling and fixation, ergonomics, and robustness have been identified in the actual model. Fixing these problems will be the next step to allow the progress of the whole project.

## 1.3 Motivations and goals

The project is currently stuck because handling the samples without damaging them using the actual container is too complicated and time-consuming, this limitation makes the tuning of laser parameters highly complex. For this reason, a brand-new design for the container and a suitable workflow is necessary to ensure perfect repeatability during the ablation of the samples. Therefore, the main aim of the thesis project is to conceive and manufacture the aforementioned container towards higher intuitiveness and better usability especially for novice users. After that, validation of the proposed solution will be carried out to check the real impact of the modifications through customized experiments on samples that do not require sterile conditions. The major requirements that must be satisfied are both engineering and biological, complying with them will be the driving force of the entire thesis project:

- Biocompatibility of the container
- Sterility during the process
- Clear path from the laser source to the samples
- User-friendly design
- Ergonomic handling of the samples
- Adaptability to different setups

At the moment, the aim of designing this new container is basically to have a transportable sterile environment to move the samples around without damaging or contaminating them during different experiments. In the future, the work carried on during this six-month-long thesis could lay the foundations for further developments and maybe, one day, refreshing the cartilage defects using laser ablation will become the standard procedure.

## 2 Literature review

In this chapter, the main aspects of the initial literature review are briefly summarized for a better comprehension of the whole work and to show the actual state of the art in this field.

### 2.1 Osteoarthritis

Osteoarthritis is a type of joint disease that mainly affects the cartilage of joints [7]. Cartilage is the slippery tissue that covers the ends of bones in a joint, and it helps them move smoothly. In osteoarthritis, the cartilage begins to break down and wear away, causing the bones to rub against each other. This can cause pain, stiffness and in advanced stages muscle atrophy and limb deformity. Osteoarthritis can affect any joint in the body and can be divided into two types: primary (typically related to aging and wear and tear on the joints) and secondary (usually caused by an underlying condition or injury that damages the cartilage in the joint). It is a progressive disease that gets worse over time, and it is more common in older adults. The exact cause of osteoarthritis is not known, but it is believed to be a combination of genetic, environmental, and lifestyle factors. There is currently no cure for osteoarthritis, but treatments can help manage the symptoms and improve quality of life. In severe cases, joint replacement surgery may be necessary.

### 2.2 Drawbacks of current techniques for cartilage repair

The capacity of self-repair of cartilage in the knee joint is extremely low, no blood vessels reach the tissue and the healing process depends on blood from the below subchondral bone. Different treatments are today available for cartilage defects [8]. One potential option is microfracture surgery, the procedure stimulates fibrocartilaginous tissue to grow into the defect and cover the underlying bone. However, this technique could further damage the cartilage if not performed correctly and the success of the operation is strictly related to the skills of the surgeon. Another one consists of lavage and debridement to eliminate loose scraps of cartilage but its effect is just palliative and temporary. Finally, the most complex method is based on filling the cartilage defects through autografts produced from debrided tissue collected arthroscopically around the lesion. Nevertheless, this technique shows various drawbacks like the incongruity of the plug or the health of the chondrocytes that could be affected by the same alterations of the surrounding cartilage.

### 2.3 New kind of grafts

A new promising method has been conceived thanks to the synergy between an innovative source of healthy chondrocytes and the principles of tissue engineering. Some studies have pointed out the higher and more reproducible chondrogenic potential of nasal chondrocytes compared to knee ones [9], nasal chondrocytes show a superior proliferation rate and a better tendency to chondro-differentiate. The autologous grafts made starting from this new source have a more resistant and robust matrix thanks to the more significant amount of glycosaminoglycans and type II collagen [10], in other words, this new kind of graft should be able to better perform after being implanted and last longer than a graft made with knee cells. The first human trial has shown positive results, radiological assessments performed 24 months after the surgery indicated good degrees of defect filling and development of repair tissue without observing adverse reactions.

## 2.4 Laser ablation

Before the graft is implanted in the cartilage, the defect needs to be refreshed to remove the damaged tissue and provide a clean layer to attach the graft. Today, this operation is made by surgeons through biopsy punches and surgical knives in a complete mechanical approach. Even if this method is straightforward and affordable, there are various disadvantages like the cut's low precision level, the damage to the surrounding tissues [11], alterations in terms of cell viability or lack of reproducibility. A valid alternative to avoid these problems is the use of specific models of laser that release an amount of energy suitable for the ablation of biological tissue. The overall effect of laser ablation is related to the features of the laser (wavelength, pulse duration, beam quality, repetition rate, intensity) and the characteristics of the target tissue (water content, optical properties, chemical composition), however, the consequences of different combinations of these parameters have been studied principally on hard tissues [12]. The most common interactions between tissue and laser can be distinguished according to different values of power density and exposure time [1] (see figure 3.8):

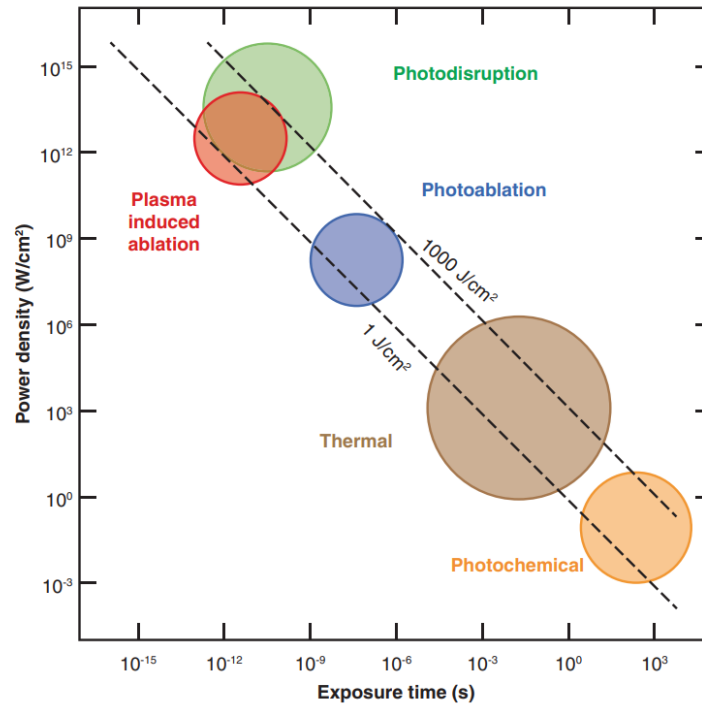


Figure 2.1: Laser-tissue interaction map depending on power density and exposure time [1].

- Photochemical interaction: Laser light induces chemical effects and reactions in the macromolecules of the irradiated tissue, it is used principally in photodynamic therapies.
- Photothermal interaction: It happens when laser light increases the local temperature of the tissue. Depending on the achieved temperature peak, this mechanism can be subdivided into coagulation (between 60 °C and 100 °C), vaporization (between 100 °C and 150 °C), carbonization (between 150 °C and 300 °C) and melting (over 300 °C).
- Plasma-induced ablation: The tissue is subjected to a high-intensity electric field that leads to the optical breakdown and the creation of plasma in the focal volume of the laser beam. Ablation is caused subsequently by plasma ionization in a very clean and precise way, without thermal or mechanical damage.
- Photo-disruption: This phenomenon is a direct consequence of plasma formation, high-energy plasma creates shock waves that break apart the tissue, moreover other side events, like cavitation and jet formation, can also take place because of gaseous vapor and CO<sub>2</sub>. The effects of photo-disruption can spread to surrounding tissues, unlike in the aforementioned mechanisms.

## 2.5 Laser ablation of cartilage tissue

Most of the studies about tissue ablation are about the ablation of hard tissues like bones or teeth, on the contrary, the papers about the interaction between laser beams and cartilage tissue are limited. The first experiments have been realized to understand how laser light can affect the mechanical properties of the cartilage. The compressive modulus of cartilage ranges between 1.24 MPa (femur cartilage) and 0.45 MPa (tibial plateau cartilage) in the human body [13], this value decreases considerably resulting in a more flexible structure when the tissue is irradiated by Nd:YAG laser [14]. In the last few years, at DBE of the University of Basel, some studies have been undertaken to evaluate the real advantages of using laser cutting instead of surgical tools to reshape cartilage tissue. However, this research is still ongoing and the results are not definitive. Initially, analyzing the outcomes during a short timeframe of just 24 hours, it has been demonstrated that cell viability is superior when the cut is performed with an Er:YAG laser instead of surgical scissors [2]:

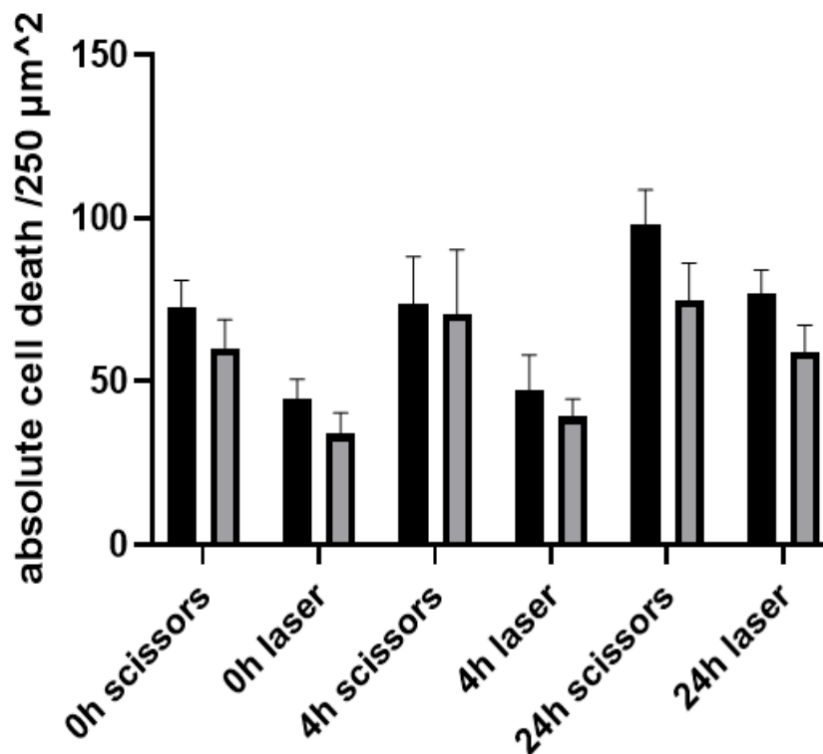


Figure 2.2: Cell viability after laser and surgical scissors reshape in surrounding tissues 0-200  $\mu\text{m}$  (black bars) and 200-400  $\mu\text{m}$  (grey bars) distant from the cutting edge at different times [2].

As shown in figure 2.2 the number of dead cells around the incision line is consistently higher if the cut is realized with surgical tools. However, this analysis has been conducted on a restricted number of samples and over a brief period of time to consider the results definitive. In another experiment, the quantitative results of the immunohistochemical analysis at the protein scale showed that the biopsy punch caused increased MMP-13 (the key enzyme in the cleavage of type II collagen) level compared to the laser ablation [15]. In this case, the focus was on gene expression of the cells surrounding the cut and the time span was extended from 24 hours to one week. These two parallel studies are in some ways complementary and show encouraging signs for future discoveries in this field. The next step is to understand if refreshing the defects using laser ablation instead of surgical tools improves the goodness of the integration between the graft and cartilage. Various experiments will be necessary for this scope, as well as a new container for the samples to ease the procedures.

## 3 Methods

### 3.1 Requirements

First of all, it was necessary to define the requirements that the container has to comply with to be used safely and without damaging the samples. These requirements have been discussed firstly with the LAROCARE project members who have designed the old model, to understand what kind of problems they encountered during the previous experiments. The next step was deciding the shape and dimensions of the samples and this aspect was discussed with the biologists of the DBM. In the end, the optic experts of the BLOG have underlined the issues that have to be taken care of to optimize the laser ablation during the experiments.

#### 3.1.1 Meeting with DBM biologists

The meeting with the DBM biologists, in particular with Prof. Andrea Barbero, was scheduled to define the shape of the samples that will be used to perform laser ablation inside the new container. The meeting took place in the Biomedicine department of the Universitätsspital Basel, where Prof. Barbero and his team conducted their research. The team receives almost every week bone specimens from surgical knee replacements performed in the previous days. The amount and quality of the knee tissue depend on the specific patient and on the surgeon's experience. Moreover, depending on the kind of prosthesis that will be implanted, the sample could contain the whole joint (two condyles and the tibial plateau, in total prosthesis replacements) or just a part (one condyle, in resurfacing prosthesis replacements). See figure [3.1](#).

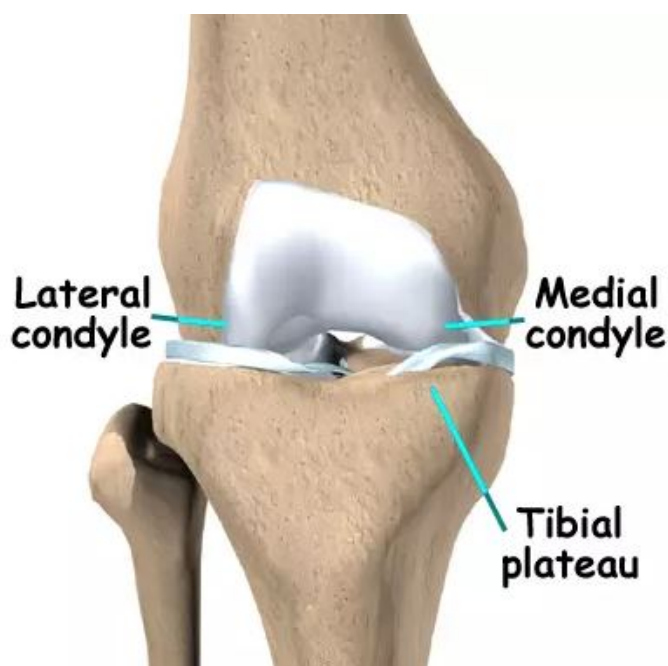


Figure 3.1: Anatomy of the knee joint. The femoral condyles are the two rounded prominences at the end of the femur, the tibial plateau is the flat top portion of the tibial bone.



The figure [3.2](#) shows the whole specimen obtained from a total knee replacement surgery performed on a 78-year-old patient.

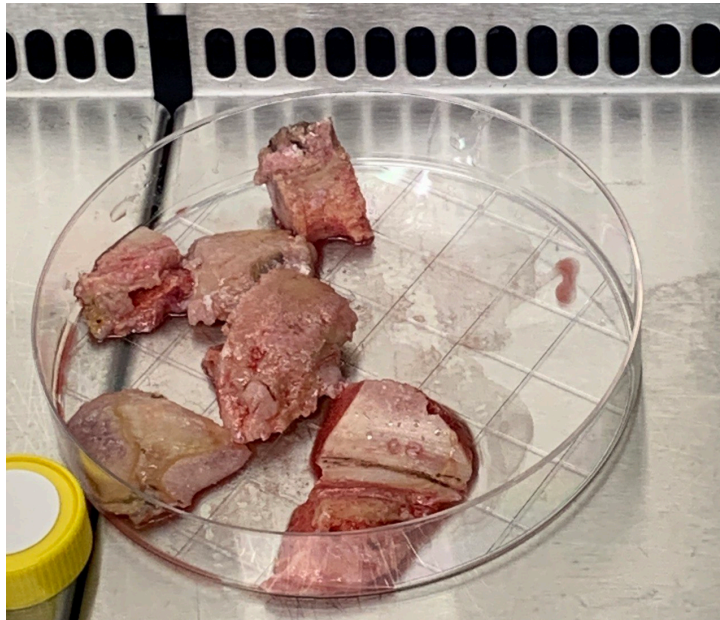


Figure 3.2: Picture of the entire knee joint sample harvested during surgery.

Starting from the entire sample, it is necessary to select the bone tissue still covered by cartilage, while the rest of the tissue can be removed. In this case, the joint was so ruined that only the tibial plateau was still partially covered by healthy cartilage. Instead, the condyles were completely degenerated and unusable for this scope. In figure [3.3](#) are shown the parts of the joint actually used.

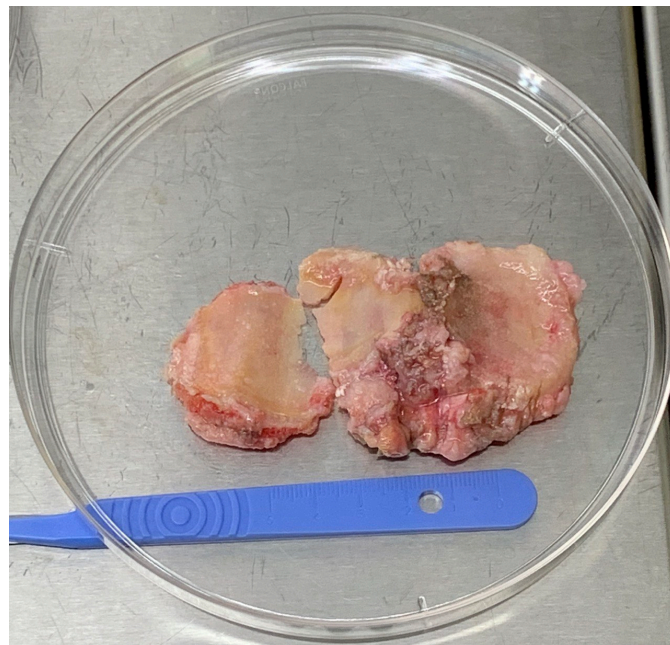


Figure 3.3: Picture of the tibial plateau extracted from the whole sample.

The tibial plateau was broken in two pieces during the surgery and the lateral concavity was totally cartilage-free due to the advanced state of osteoarthritic degeneration. The medial concavity was still sufficiently healthy, so the final sample was harvested from this anatomic region. In figure [3.4](#) it is possible to see two different moments of the procedure.



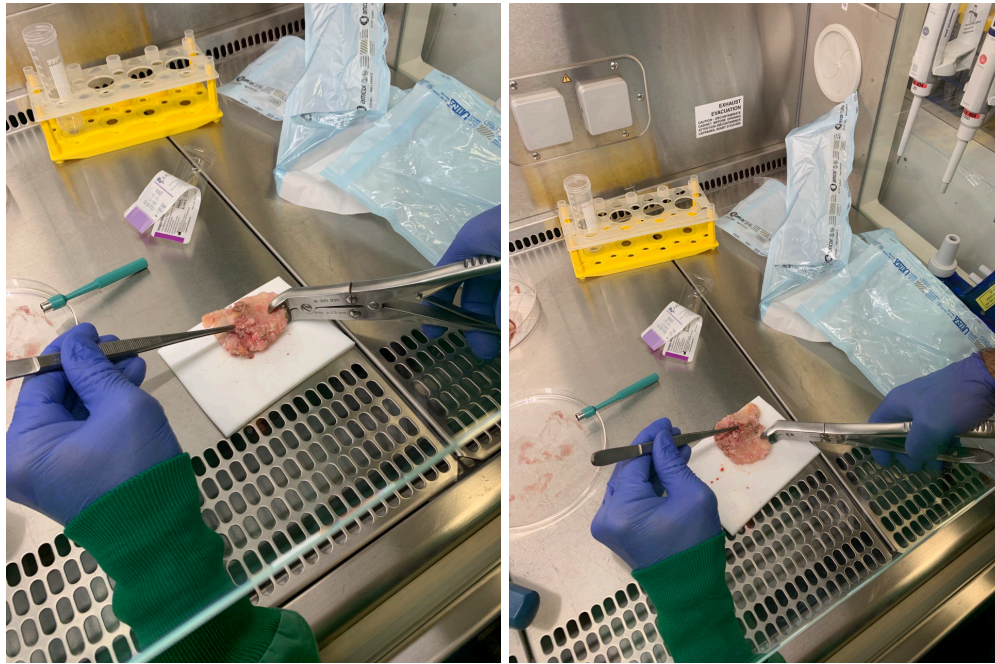


Figure 3.4: Resizing of the tibial plateau to fit inside the new container. The procedure was performed by Prof. Barbero using surgical pliers and shears.

The ultimate result is a piece of bone tissue covered by alive cartilage with an approximately circular shape (see figure [3.5](#)). The diameter of the sample is about 2 cm and it will be placed inside the new container and laser ablated. Only one sample was extracted during the first meeting, however, the plan is to design a container that can contain multiple samples at the same time. The main drawback of the procedure is the inability to create standardized samples because of the difficulties in cutting extremely stiff tissue like bone using surgical tools. Moreover, the procedure could affect the viability of the sample and alter the results of future experiments.



Figure 3.5: Picture of the final sample obtained using surgical tools.

### 3.1.2 Meeting with BLOG laser physicists

This meeting was held inside the BLOG laboratory, a properly equipped work environment where the lasers can safely perform ablation experiments with different purposes. The properties of the two available lasers for tissue ablation were the main focus of the discussion (see Table 3.1), together with the geometrical and functional requirements for the new container.

- Nd:YAG pulsed laser (Q-smart 450, Quantel Technologies, Les Ulis, France): realizes plasma-induced ablation with a pulse duration of 5 ns and an adjustable pulse energy in the range of 2 to 170 cm. It works at a wavelength of 532 or 1064 nm, so its light is hardly absorbed by aqueous solutions. For this reason, its primary use is the preparation of live samples which need to stay inside a nutrient liquid during the process. Another reason to ablate tissue inside an aqueous environment can be to ensure constant cooling to the ablation site, which decreases the risk of laser-induced thermal damage (see Figure 3.6).



Figure 3.6: Picture of the Nd:YAG pulsed laser.

- The Er:YAG pulsed laser (Lite-Touch, Syneron Medical Ltd., San Francisco, CA): it operates at a wavelength of 2940 nm and its beams are highly absorbed by water, rendering it more adequate for dry samples. It realizes photothermal ablation, features a pulse duration in the order of microseconds and delivers a maximum pulse energy of 1000 mJ (see Figure 3.7).

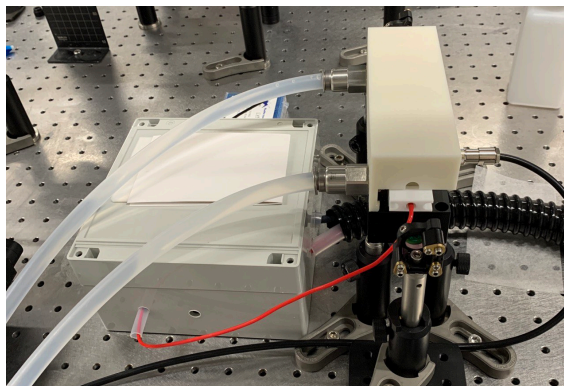


Figure 3.7: Picture of the Er:YAG pulsed laser.

Table 3.1: Specifications of the two aforementioned lasers.

Laser	Wavelength (nm)	Pulsed energy (mJ)	Pulse duration ( $\mu$ s)	Ablation mechanism
Nd:YAG pulsed	532 or 1064	2-170	0.005	Plasma-induced ablation
Er:YAG pulsed	2940	<1000	100-400	Photothermal ablation

## 3.2 First list of requirements

All the needed requirements that emerged from these three different meetings are discussed in the list below and summarized in Table [3.2](#)

- **Biocompatibility:** All the inside components of the container must be completely biocompatible, not only the parts that are directly in contact with samples. Within the container, there is a nutrition liquid that keeps the specimens hydrated and alive during the process. Some toxic particles could reach the samples through the liquid, even if the toxic materials are not directly in touch with the samples. Obviously, in that case, the outcome of the experiment would be altered because the effects generated by the laser ablation would be mixed up with the effects caused by the cytotoxic components.
- **Sterility:** The sterility inside the container must be guaranteed from the initial positioning of the samples until the extraction after the ablation. From the moment that the lasers are in an unsterile environment, the container cannot be opened during the experiment and every movement of the samples has to be implemented from the outside. Air-tightness and water-tightness are strictly required to avoid contamination. Furthermore, the container must be autoclaved before every experiment and, for this reason, it has to be realized in heat-resistant materials that can bear temperatures over 120 °C.
- **Laser transparency:** The two lasers mainly used in the field of tissue ablation are Nd:YAG laser and Er:YAG laser which can work respectively with a wavelength of 532 nm or 1064 nm for the first and 2940 nm for the second. However, not every kind of glass is transparent to these specific wavelengths. Using a glass that partially absorbs the laser light would drastically reduce the amount of energy transferred from the laser source to the sample, decreasing the efficiency and precision of the ablation. Moreover, condensation and ejected debris from the tissue can also obstruct the laser path through the glass window.
- **Ergonomy:** The design of the new container should be as ergonomic as possible to handle the samples without damaging them. Biologic tissues are very brittle, especially bone, so the positioning of the sample has to be achieved by applying small pressure, otherwise, apoptosis could be induced in the cells by mechanical stresses. Besides, moving the sample in and out from the nutrition liquid has to be simple and quick.
- **Adaptability:** The outcome of an experiment based on laser ablation strictly depends on the laser parameters and on the conditions of the sample, in most cases, finding the right mix between them requires a trial-and-error approach. For this reason, changing the setup of the experiment might be necessary and the container has to be easily adaptable to different configurations. Also, the container's shape and overall dimension must be suitable for different setups.
- **User-friendliness:** Filling up the container with the sterile samples will be likely performed in anticontamination safety rooms by members of the medical staff. The same people have to clean the container of tissue residues after the experiment. These people were not involved in the modeling of the container. To ease their work, high intuitiveness and a simple assembling procedure complete the picture of the needed requirements. At the same time, having the possibility to watch inside the container is essential to ease the work during the ablation.

Table 3.2: First list of requirements for the new container.

General requirements	Derived requirements
1. Biocompatibility	Anti-cytotoxic materials Materials suitable for nutrition liquid
2. Sterility	Air-tightness Water-tightness Autoclavable materials Sealable opening
3. Laser transparency	Transparent window for light with a wavelength between 532 and 2940 nm Anti-condensation system Anti-debris design Mechanism to extract the sample from the liquid
4. Ergonomy	Easy sample insertion Quick sample positioning Stable and harmless sample fixation Reproducible positioning Two degrees of freedom sample movement At least 2x2 cm for every sample Modular design
5. Adaptability	Several available samples Rectangular bottom Max dimensions 30x30x30 cm Max overall weight of the container 5 kg Platform able to support 1 g heavy sample
6. User-friendliness	Highly intuitive assembling procedure Visible inside mechanism Drop robustness



### 3.3 Old container

After having defined the necessary requirements, the next step was analyzing the old container in order to underline the advantages and take note of the critical issues related to its design. The study of the old model will be the starting point for the design of the new one.



Figure 3.8: Picture of the old container, completely assembled. The total height is about 26 cm and the diameter of the bottle is approximately 10 cm.

### 3.3.1 Components

The old version of the container shown in figure 3.8 was not designed from scratch but it was created by assembling different components which originally had different purposes 4:

- **Sapphire Lid:** The top part of the container is composed of the lid of the bottle embedded through some screws with a cage plate (LCP01T/M, Thorlabs, Inc., Newton) that is designed to hold a glass window (WG31050, Thorlabs, Inc., Newton). The window is made of sapphire glass because this material is transparent to the wavelengths of the lasers (See Figure 3.9).



Figure 3.9: Pictures from two different points of view of the sapphire lid, the diameter of the sapphire window is around 5 cm.

- **Glass bottle:** The main part of the container is realized using a standard sealable wide-neck laboratory glass bottle (9.284 523, Faust Laborbedarf AG, Schaffhausen, Switzerland). The bottle is impermeable, transparent and it has an inner volume of more or less one liter to contain the sample and the nutrition liquid (See Figure 3.10).



Figure 3.10: Picture of the glass bottle.

- **Sample holder:** It is composed of a stainless steel net and eight ferrite magnets (four directly attached to the net and four outside of the bottle). The sample can be positioned on the net and kept still using some metallic clips, the structure can be moved from the outside using the magnets to align the sample with the laser light (See Figure 3.11).

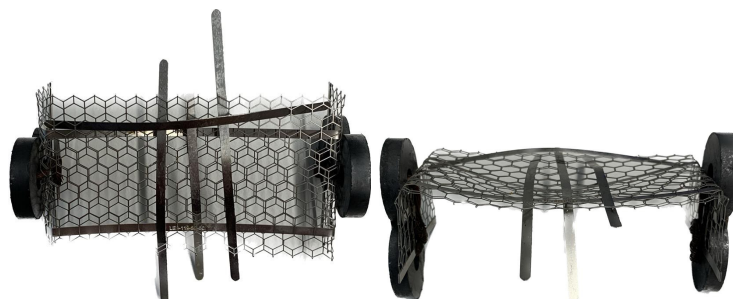


Figure 3.11: Pictures from two different points of view of the sample holder.

### 3.3.2 Pros and cons

The container was successfully used in the previous experiments carried on by the LAROCARE project members during which it complied with the mandatory requirements for the ablation process. However, this design showed a lot of intrinsic limitations that led the team to opt for a new model:

- **Biocompatibility:** In terms of biocompatibility, the container has shown good properties. All the inner components were made using noncritical materials (glass, polypropylene, silicone and stainless steel) and the samples did not manifest severe reactions during or after the experiments. The only issue was related to the presence of the magnets. High-strength neodymium-iron-boron magnets could not be used because of their moderate cytotoxicity. For this reason, ferrite magnets were chosen, even if they are weaker than the others and still have a low degree of cytotoxicity. In the actual design, the inner magnets are necessary to position the sample, however, they inevitably release toxic particles in the nutrition medium. In the future version, a new mechanism to move the sample needs to be implemented to avoid the use of magnets and increase the overall level of biocompatibility.
- **Sterility:** The container was perfectly able to keep sterile the inside environment, no signs of contamination were found analyzing the sample after the ablation. The glass bottle was already realized to be impermeable. However, some silicon rings were used to fill the custom holes created after the addition of the cage plate. Furthermore, all the parts are sufficiently heat-resistant to be autoclaved without any damage.
- **Laser transparency:** The two aforementioned lasers available in the LAROCARE project use beams with wavelengths between 532 nm and 2940 nm. The 5 mm thick sapphire window attached to the lid of the container is projected to have a level of transparency of around 0.9 for light beams with a wavelength from 500 nm to 4000 nm, as shown in figure 3.12. Both lasers can reach the sample through the sapphire window with sufficient power to perform the ablation and only a small portion of the emitted energy is lost along the path from the source to the target. From this point of view, the solution is optimal, however, the sapphire window can be sometimes obstructed by condensed water or tissue debris. Moving the container from the biosafety room to the laser lab causes a sudden decrease in the ambient temperature, which cools down the inside air near the window, leading to the condensation of some of the water contained therein. As regards the debris, they are generated during the ablation (see Figure 3.13) from micro-explosions of tissue. If the eviction is too violent, the debris can reach the sapphire glass and stick to it. So, during the modeling of the new container, one of the goals will be to take care of these two issues.

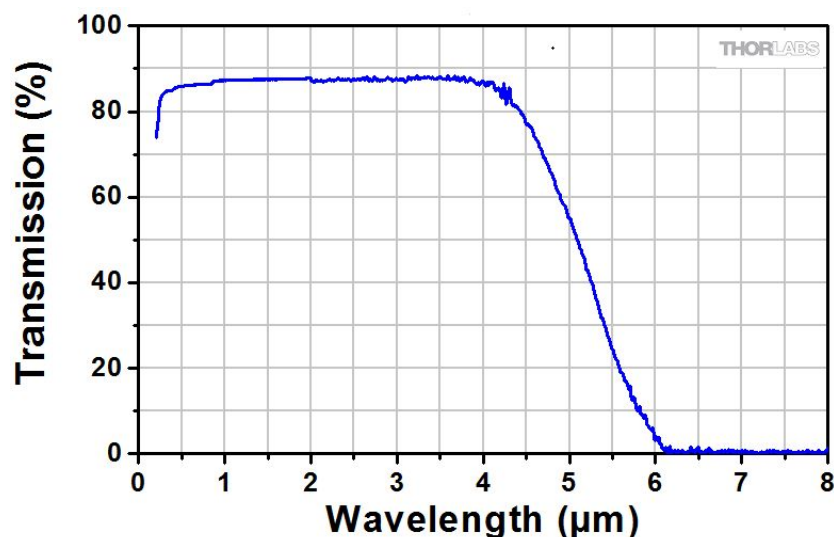


Figure 3.12: This plot gives the measured total transmission of the 5 mm thick sapphire window.

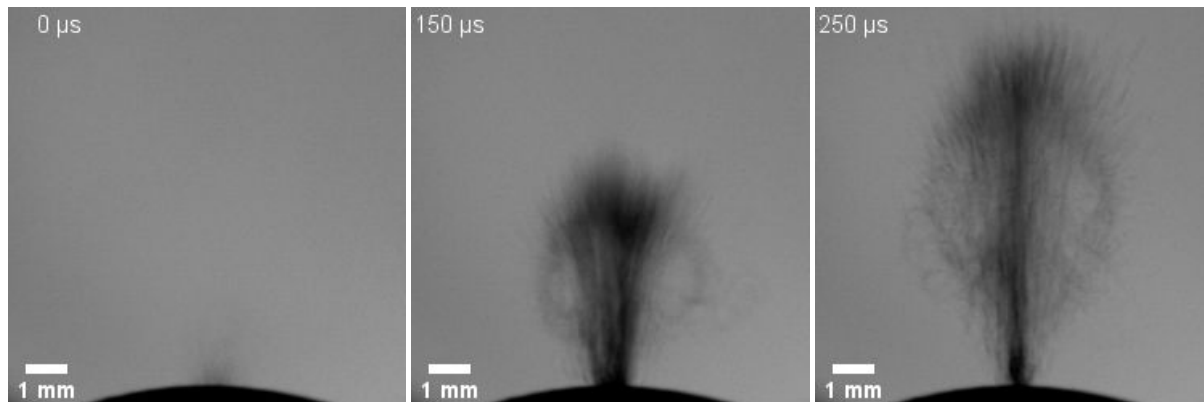


Figure 3.13: Debris expulsion during laser ablation in three different moments.

- **Ergonomy:** The main issues related to the old container come from a total lack of ergonomy during the positioning of the sample. The tissue is initially attached to the stainless steel grid through some adjustable clips, then it is inserted inside the bottle glass and the container is sealed by the lid. During the insertion, the sample could be damaged because the neck of the bottle is too narrow for the grid. The bending of the metallic net can cause unphysiological pressures on the tissue and alter cell viability. Once the container is sealed and it is taken outside the biosafety room, the sample can be moved only through the magnets. This aspect can heavily affect the success of the experiment, it is practically impossible to standardize the position of the sample by hand, whereby the reproducibility of the ablation cannot be assured. Furthermore, if the sample detaches from the grid, it cannot be repositioned until the container is inside the biosafety cabinet. Finally, the weakness of the magnets makes manipulating the grid highly difficult and time-consuming. From these considerations, it is clear that the remodeling of the container will start right by solving the ergonomic issues.
- **Adaptability:** From the moment that the optimization of the laser parameters requests a trial-and-error approach, having the possibility to ablate different samples during the same experiment would be very useful. Unfortunately, the actual container does not provide sufficient space for more than just one or two samples depending on their dimensions. Besides, the shape of the bottom of the glass bottle is not suitable for the platforms of the laser lab. Therefore, the next container will need a new shape and better inside space management.
- **User-friendliness:** Without problems regarding the ergonomy, the procedure to assemble the container would be highly easy and quick. The design is extremely simple and everyone can immediately understand how to place in position the sample. Nevertheless, from a practical point of view, there may be some difficulties because of the risk of damaging the tissue.

Therefore, this project will aim to develop a container able to combine the useful features of the old model with new ideas to better meet all the needed requirements. As discussed, some components of the first version are already optimal (see Table 3.4) and represent a good starting point for future improvements.



Table 3.3: Requirements with which the old container complies (green) or does not comply (red) from the first list.

General requirements	Derived requirements
1. Biocompatibility	Anti-cytotoxic materials Materials suitable for nutrition liquid
2. Sterility	Air-tightness Water-tightness Autoclavable materials Sealable opening
3. Laser transparency	Transparent window for light with a wavelength between 532 and 2940 nm Anti-condensation system Anti-debris design Mechanism to extract the sample from the liquid
4. Ergonomy	Two degrees of freedom sample movement Easy sample insertion Quick sample positioning Modular design Stable and harmless sample fixation Reproducible positioning At least 2x2 cm space for every sample
5. Adaptability	Several available samples Rectangular bottom Max dimensions 30x30x30 cm Max overall weight of the container 5 kg Platform able to support 1 g heavy sample
6. User-friendliness	Highly intuitive assembling procedure Visible inside mechanism Drop robustness

### 3.4 Design process

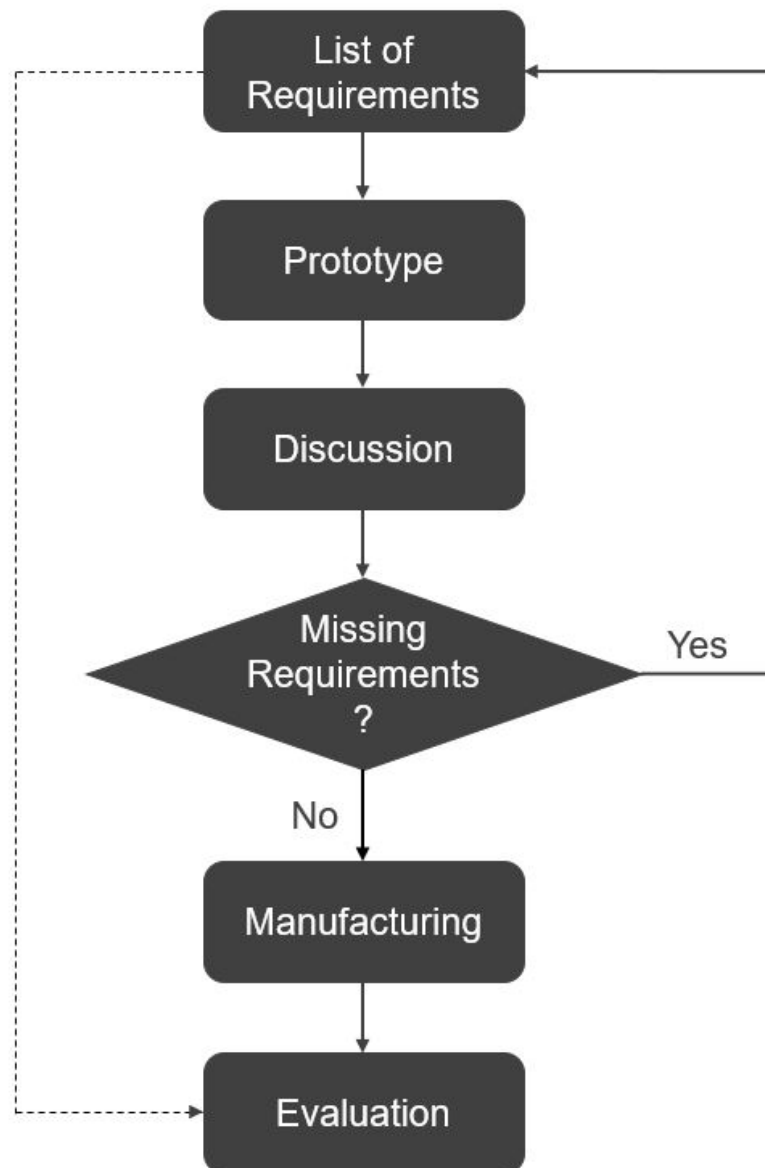


Figure 3.14: The picture shows the flowchart followed during the design process.

The flowchart shown in Figure [3.14](#) describes the process that was applied during the design phase. The first step is to list the requirements that are deemed necessary to successfully perform laser experiments using the new device. Based on this list, a prototype is accordingly designed and discussed. The discussion is carried out together with the members of the LAROCARE Project and the aim is to understand if there may be some issues that were not considered at first. At this point, if the list is still believed incomplete, it will be updated and a new prototype has to be thought up. Instead, in the other scenario, the prototype can be actually manufactured through autoclavable and biocompatible materials. Once the final device has been manufactured, it is evaluated to assess compliance with the current list of requirements.

## 3.5 First prototype

The first proposed design for the new container was based on the list of requirements previously described, the aim was to comply with the most number of them using cheap and not autoclavable materials. Then, if the model was deemed suitable by future users, it would have been produced again with proper materials to make it resistant to high temperatures. Even if this prototype is deeply different from the final model, it is worth to be described for three main reasons: the techniques and the methods used to create it are the same that have been used to manufacture the succeeding prototypes, it helped to figure out how to refine the approach for cartilage sample ablation and its analysis was fundamental to update the set of requirements.

### 3.5.1 Designing and prototyping

The prototype was first designed using Solidworks, it was composed of two main parts: the inner rotational mechanism and the external box. The 3D design can be seen in Figure [3.15](#)

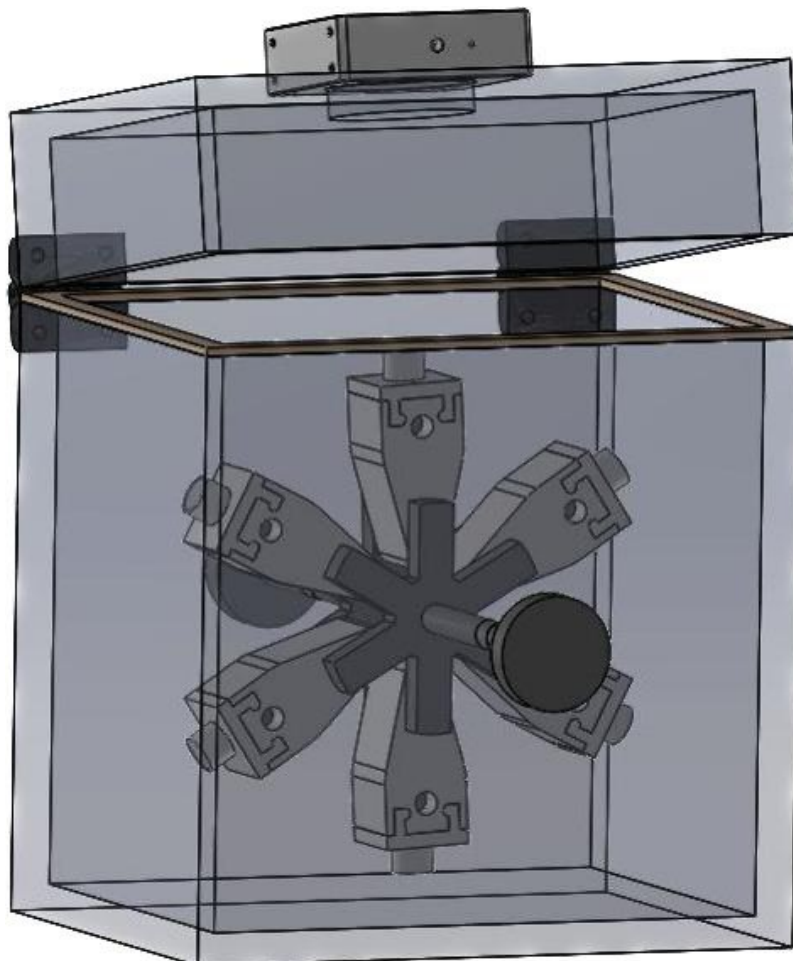


Figure 3.15: The picture shows the CAD project of the first prototype.

The inner mechanism is connected to two knobs that can be controlled from the outside, these knobs are used to move six identical sample holders along a circular path and to tilt them relative to their vertical axis. This kind of double movement is allowed by the relative motion between every sample holder and two pins directly linked to the external knobs. The outside box can be opened through two hinges and exhibits three holes, two holes to link the external knobs to the rest of the inner mechanism and one wider hole on the top that has the same diameter as the sapphire window. The cage plate is positioned on the top side to make the sapphire window and the larger hole concentric to obtain a clear path for the laser.

After that, the prototype was manufactured through laser cutting and 3D printing:

- Laser cutting was performed through Glowforge Plus (Glowforge Inc., Seattle, WA), shown in Figure 3.16, on 5 mm thick acrylic panels to obtain the walls of the external box. Then, the box was assembled using stainless steel screws and hinges.

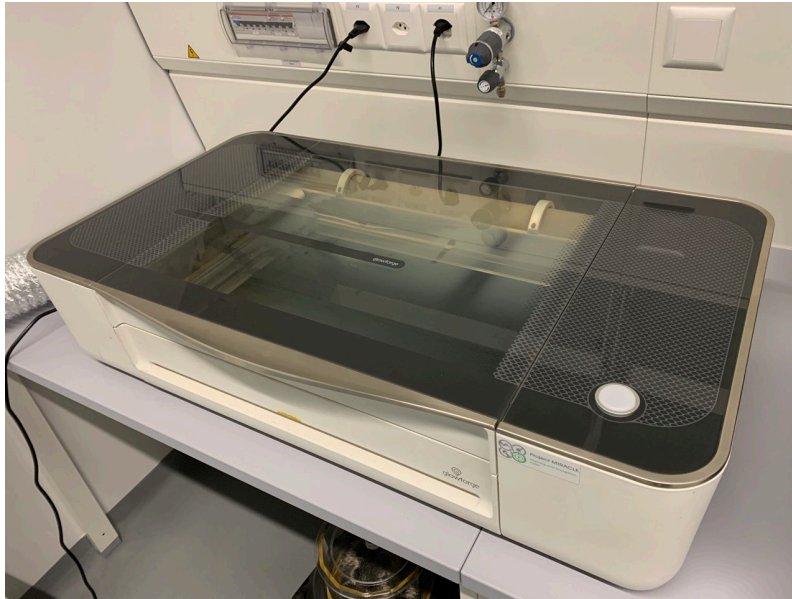


Figure 3.16: Picture of the laser cutter Glowforge Plus.

- 3D printing was performed through the printer Fortus 250mc (Stratasys Ltd., Rehovot, Israel), shown in Figure 3.17. All the components of the inner mechanism were fabricated using this device in 3D-printed material (ABSplus P430), except for the two knobs that were off-the-shelf components.



Figure 3.17: Picture of the 3D printer Fortus 250mc.

The final result is slightly different from the CAD project, as shown in Figure 3.18. The main differences are the top part of the box and the shape of the sample holders, both changes were made to simplify the design. At this point, it was not necessary to replicate exactly the ideal model but it was enough to have a simple prototype to evaluate the pros and cons. Moreover, through this simplified approach, time and material were saved. The combination of 3D printing and laser cutting is the prototyping method that will be used until the design is shown to be suitable for the final task.

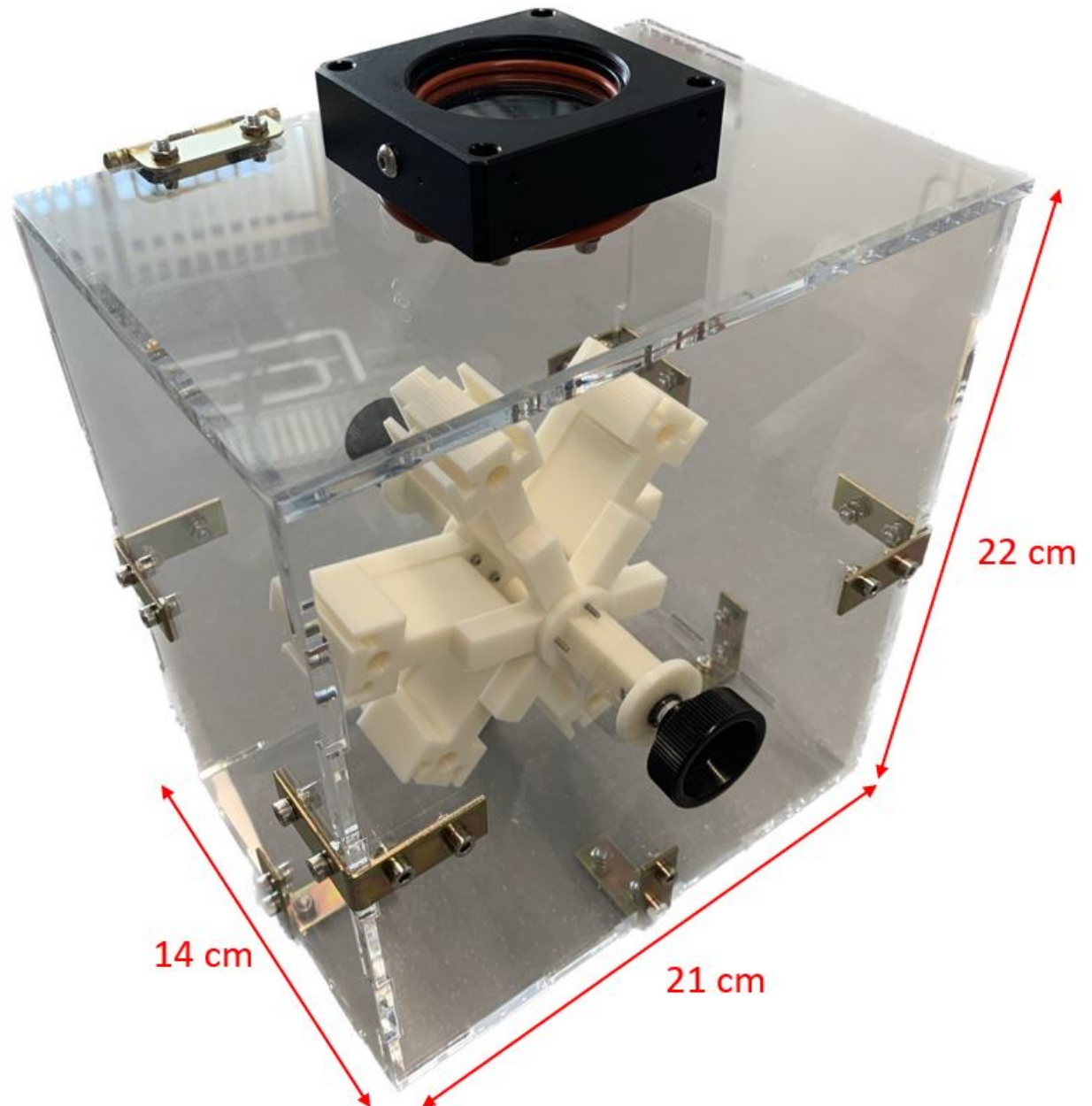


Figure 3.18: The picture shows the prototype realized in acrylic and 3D printed material. The dimensions of the box are approximately 22x14x21 cm



### 3.5.2 Pros and cons

The analysis of the first prototype was a fundamental step in improving the design of the final container, thanks to this device was possible to focus more precisely on the real needs in terms of positioning the sample, eliminating unnecessary components and defining the right overall size of the container. The main goal was to evaluate the ergonomics and ease of use of the product, without paying attention to the other issues.

- **Biocompatibility:** The inner mechanism was realized using 3D-printed material and so was the sample holder, this kind of thermoplastic material is not suitable to be in contact with live tissues. Also, it would be necessary to test if the acrylic plastic used for the box is stable when it is immersed in the nutrition liquid. In other words, the prototype cannot ensure a biocompatible environment for the cartilage sample. The main advantage of this setup is that magnets are no longer necessary, solving the issue related to their slight cytotoxicity.
- **Sterility:** Water and air tightness are assured by the use of several silicon rings to seal the holes created for the two knobs, the cage plate and the screws (see Figure 3.19). However, as expected, this prototype cannot be autoclaved because of the not heat-resistant materials.

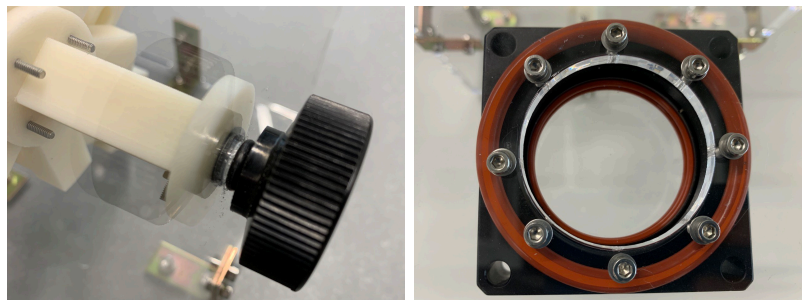


Figure 3.19: In the picture on the left it is possible to observe the black silicon ring used to seal the hole for the knob, in the picture on the right it is shown the orange ring that seals the attachment between the cage plate and the box.

- **Laser transparency:** The use of the aforementioned sapphire window allows laser beams to easily reach the sample when the sample holder is aligned with the hole on the top (see Figure 3.20), besides, the distance between the sample holder and the window itself should avoid debris deposit. The rotating mechanism is designed to extract one sample per time from the nutrition medium, thus energy dissipation caused by water is not an issue. Anyhow, a solution for the condensation problem is still required.

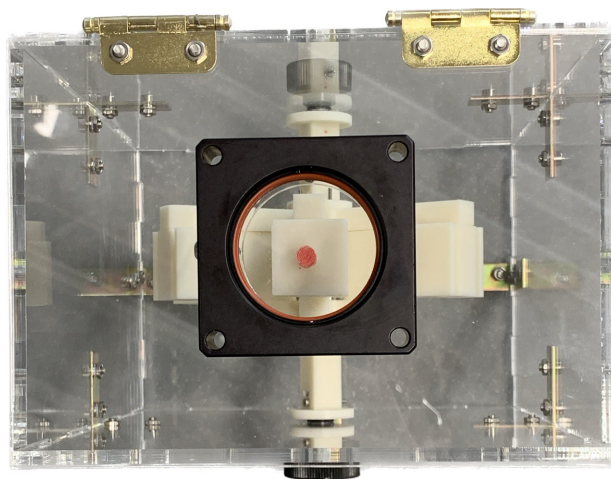


Figure 3.20: Top view of the container, the red phantom in the center of the sapphire window represents the cartilage sample.

- Ergonomy: Several solutions were applied to improve the overall ergonomy of the device. First of all, the new prototype has five spots for five different samples instead of just one as in the old model. The inner mechanism is perfectly modular and allows the user to change the sample under the laser light and tilt it at an angle of about  $25^\circ$  relative to the vertical axis in both directions (see Figure 3.21). The first kind of motion happens when the two knobs rotate simultaneously, instead the inclination is achieved when only the frontal knob rotates. Furthermore, the sample holder can be disassembled to position the sample on the specific base from the outside of the box, then it can be easily and quickly inserted into the box again. Nevertheless, a stable fixation system has still to be developed to keep the samples in position even when they are upside down.

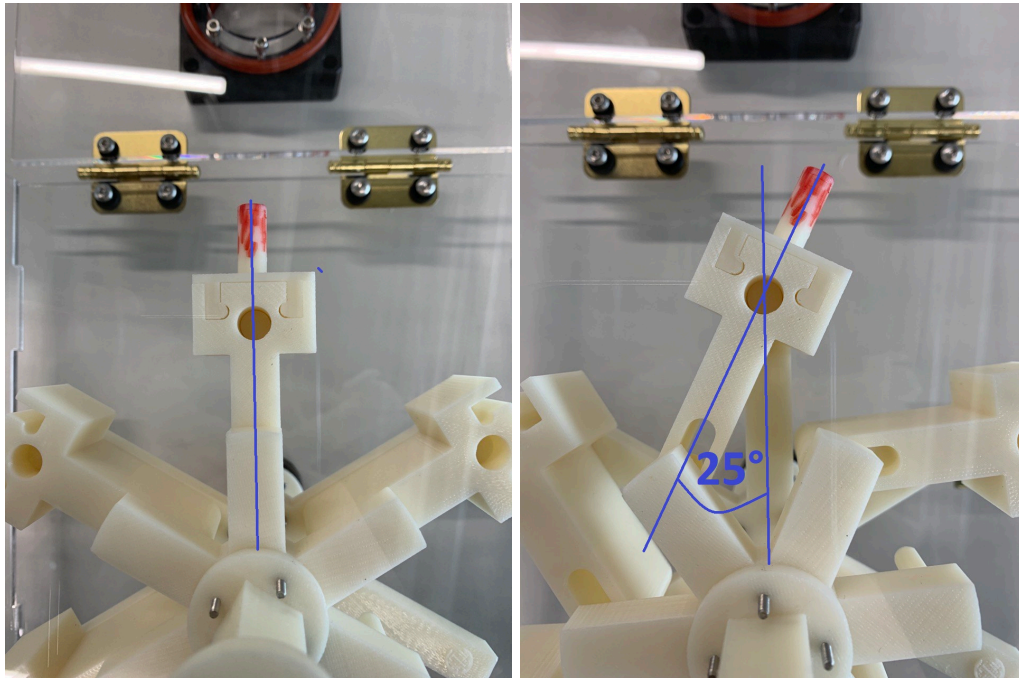


Figure 3.21: In the pictures it is shown the sample holder in two different configurations. The maximum achievable inclination in one direction is about  $25^\circ$ , which means that the overall range of motion around the rotation axis is  $50^\circ$ .

- Adaptability: The prototype will allow performing laser ablation using up to five different combinations of parameters, thanks to the five available samples. Even if there are six spots, only five of them can be actually used to allocate live samples because the sixth spot will stay outside of the nutrition medium. This is for sure the main design change compared to the old model. In terms of geometrical and dimensional properties, the prototype satisfies the remaining requirements.
- User-friendliness: Thanks to the modular sample holder, the assembling procedure is extremely easy and the risk of damaging the sample is lower. It can be executed by any healthcare professional, even if they have never seen the container before. The main issues could come from the friction between different parts, in terms of positioning and maintenance due respectively to the stick-slip effect that reduces accuracy and erosion of the components.

Looking at Table 3.4 it is clear how the prototype has improved the ergonomy and usability compared to the previous device. The first prototype could not be part of any experiment because of the materials used to build it, however, the design and realization stages were important to gain experience with 3D printing and laser cutting and to better refine the requirements for the container.

Table 3.4: Requirements with which the first prototype complies (green) or does not comply (red) from the first list.

General requirements	Derived requirements
1. Biocompatibility	<p>Anti-cytotoxic materials</p> <p>Materials suitable for nutrition liquid</p>
2. Sterility	<p>Air-tightness</p> <p>Water-tightness</p> <p>Autoclavable materials</p> <p>Sealable opening</p>
3. Laser transparency	<p>Transparent window for light with a wavelength between 532 and 2940 nm</p> <p>Anti-condensation system</p> <p>Anti-debris design</p> <p>Mechanism to extract the sample from the liquid</p>
4. Ergonomy	<p>Two degrees of freedom sample movement</p> <p>Easy sample insertion</p> <p>Quick sample positioning</p> <p>Modular design</p> <p>Stable and harmless sample fixation</p> <p>Reproducible positioning</p> <p>At least 2x2 cm space for every sample</p>
5. Adaptability	<p>Several available samples</p> <p>Rectangular bottom</p> <p>Max dimensions 30x30x30 cm</p> <p>Max overall weight of the container 5 kg</p> <p>Platform able to support 1 g heavy sample</p>
6. User-friendliness	<p>Highly intuitive assembling procedure</p> <p>Visible inside mechanism</p> <p>Drop robustness</p>



### 3.6 Second list of requirements

The first prototype was ready one month and a half after the start of the project. The requirements for the new container were discussed again using the aforementioned prototype as visual support. Having a model that complies with almost all of the requirements of the first list was fundamental for refining them and understanding how to improve the precision along the workflow. As shown before, extracting circular samples from the tibial plateau is extremely arduous and time-consuming using surgical tools, moreover, it is quite hard to standardize the final shape. For this reason, it was decided to obtain circular samples directly through laser cutting. It means that the entire tibial plateau has to be positioned under the laser light, keeping it inside a sterile environment. Hence, the inner structure of the prototype has to be deeply changed towards a new design that allows ablating a larger sample in different points, instead of ablating several smaller samples. In other words, the new model will need a single wider platform, able to move the specimen inside the container with at least four degrees of freedom, to guarantee different placements and levels of inclination. The dimensions of the new platform depend on the dimensions of the tibial plateau itself, however, they vary according to gender and age. A rough estimation of the ML (mediolateral) and AP (anteroposterior) width is extracted from [3], where the measurements were performed on a sample of 157 people through CT (computed tomography) and CR (conventional radiography) images [3.22]. As expected, men's average values were higher, besides it was noticed that the values estimated through CR were also higher than the values found using CT. For our purposes, it makes sense to consider the men's values recorded through CR as the worst-case scenario, which are  $7.54 \pm 0.61$  cm for the ML and  $4.56 \pm 0.43$  cm for the AP width. So, a rectangular platform of at least 8x5 cm will be necessary to be sure of having enough space for a wide range of different tibial plateaux.

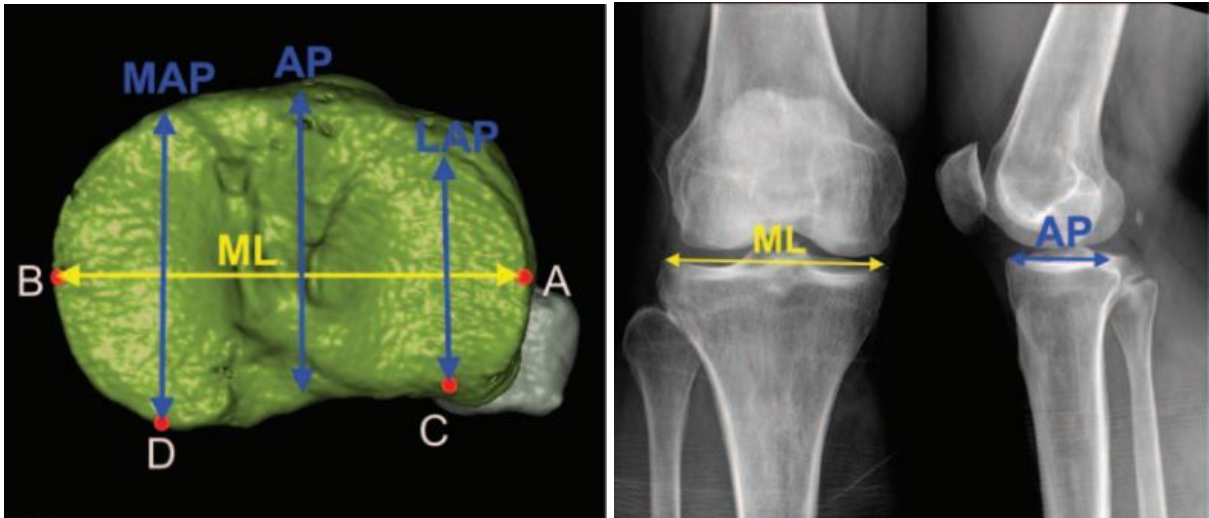


Figure 3.22: The figure shows the images from which the ML and the AP are measured, on the left the view from above of the tibial plateau generated through CT, on the right the frontal and lateral view of the knee joint obtained through CR [3].

Also, the geometrical specifications of the box were changed to increase the number of setups in which the container can be included. In particular, it was decided to decrease the overall height of the container from 30 to 15 cm. Of course, the requirements related to biocompatibility and sterility were not changed, as was the section about laser transparency, because they do not rely on the shape or size of the sample. Table [3.5] shows how the requirements changed after the prototype was discussed.

Table 3.5: Second list of requirements, the requirements that have been changed compared to the first list are written in blue.

General requirements	Derived requirements
1. Biocompatibility	Anti-cytotoxic materials Materials suitable for nutrition liquid
2. Sterility	Air-tightness Water-tightness Autoclavable materials Sealable opening
3. Laser transparency	Transparent window for light with a wavelength between 532 and 2940 nm Anti-condensation system Anti-debris design Mechanism to extract the sample from the liquid
4. Ergonomy	Four degrees of freedom sample movement (two rotational, two translational) Easy sample insertion Quick sample positioning Modular design Stable and harmless sample fixation Reproducible positioning At least 8x5 cm space for tibial plateau
5. Adaptability	Entire tibial plateau available Rectangular bottom Max dimensions 15x18x18 cm Max overall weight of the container 5 kg Platform able to support 50 g heavy sample
6. User-friendliness	Highly intuitive assembling procedure Visible inside mechanism Drop robustness

## 3.7 Second prototype

The second prototype was built through the same techniques used for the first one (laser cutting and 3D printing), however, the design is completely different. Shortly, the first device was designed to have the possibility of ablating several small samples, on the contrary, the second container aims to perform different ablations on the same larger sample. So, in the first case, the main issue was finding a way to position different samples under the laser source at different moments and, if necessary, change their tilt. In the new scenario, the entire tibial plateau has to be moved along a plane parallel to the sapphire window to perform the ablation in different regions of the sample, then it might be required to vary the spatial orientation because of the irregular surface.

### 3.7.1 Designing and prototyping

Every component of the prototype was designed again through Solidworks and then assembled to create the device in Figure 3.23. It is composed of two main parts: the box that will contain the sample and the external reservoir for the nutrition fluid.

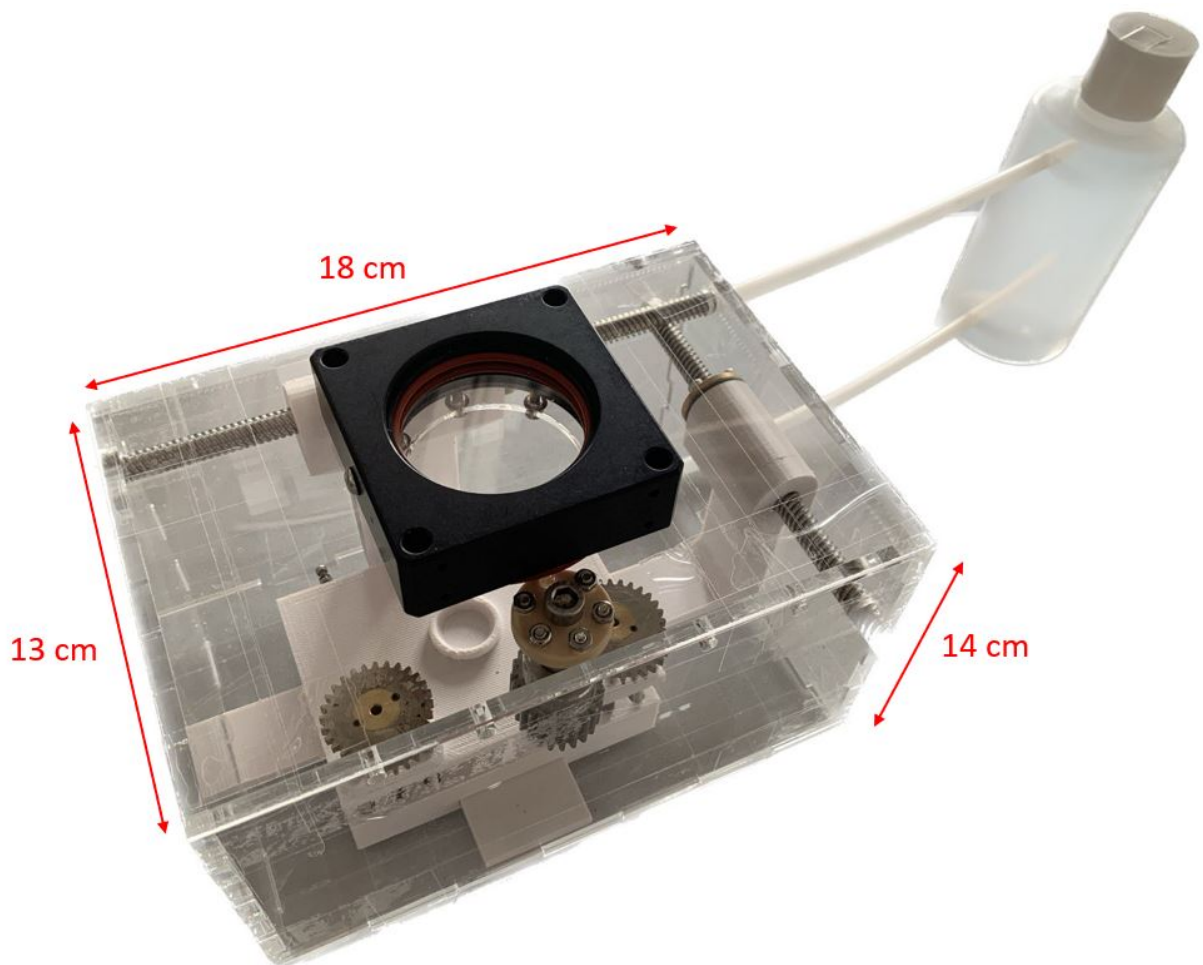


Figure 3.23: The picture shows the second prototype. The dimensions of the box are approximately 14x13x18 cm and the reservoir has a volume of 0.4l.

To ease the understanding of the following descriptions of how the new prototype achieves the four needed degrees of freedom, it is worthwhile to start describing the platform on which the sample will be placed (see Figure 3.24). The platform is composed of two rectangular parts, the lower part will be called the base while the upper one will be named the sample holder. Initially, the role of the various components may not be clear, however, it will become clearer once the rest of the prototype is properly described.

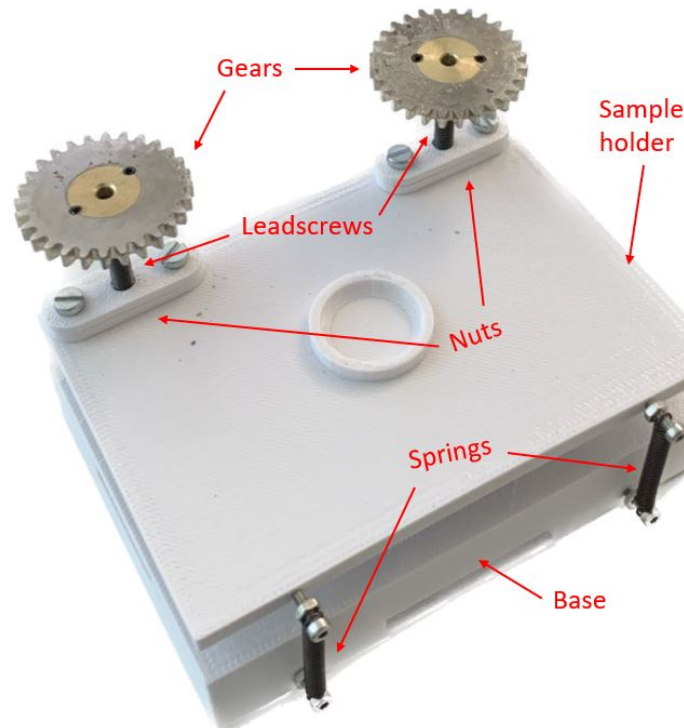


Figure 3.24: The picture shows the platform meant to hold the sample during the laser ablation.

The base is characterized by two perpendicular slots with a rectangular shape. Between the base and the sample holder, there is a spherical joint and they are kept together through two leadscrews and two springs (see Figure 3.25). Furthermore, two nuts are embedded in the sample holder and able to slide over the leadscrews. Finally, two gears are fixed on the tips of the two leadscrews. This kind of structure allows the sample holder to change its spatial orientation and keep it steady thanks to the rotation of the gears and the force developed by the springs. In fact, Without the springs, the sample holder would detach from the base because the spherical joint is not fixed. Besides, the backlash due to the leadscrews is removed, increasing the repeatability.

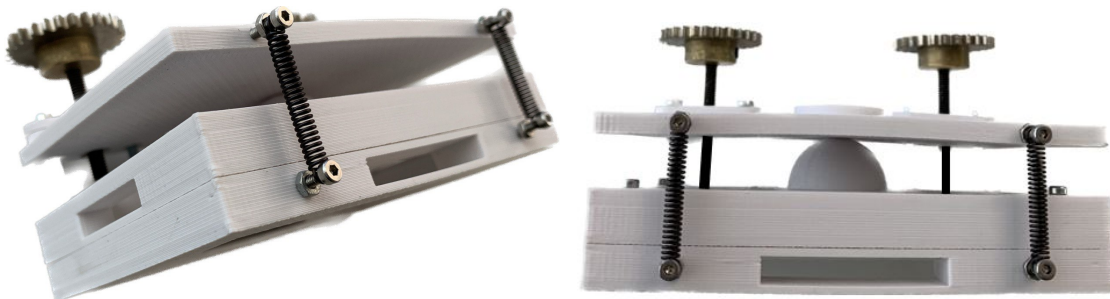


Figure 3.25: On the left the rectangular slots on the sides of the base, on the right the spherical joint that couples the base and the sample holder.

The inner mechanism is definitely more complex than the mechanism of the previous prototype and it is composed of two stages that allow to achieve two degrees of freedom each for a total of four. Given that the sapphire window is fixed and has a diameter of approximately 4.5 cm, we need to move the 9x6 cm wide platform in the  $xy$ -plane (see Figure 3.27) with a range of motion of respectively 7 cm along the  $x$ -axis and 4 cm along the  $y$ -axis to reach every corner with the laser beams. In other words, we need two translational degrees of freedom in the  $xy$ -plane characterized by the aforementioned ranges of motion along the axis. Only in this case, we can be sure that every region of the sample can be ablated without opening again the box.

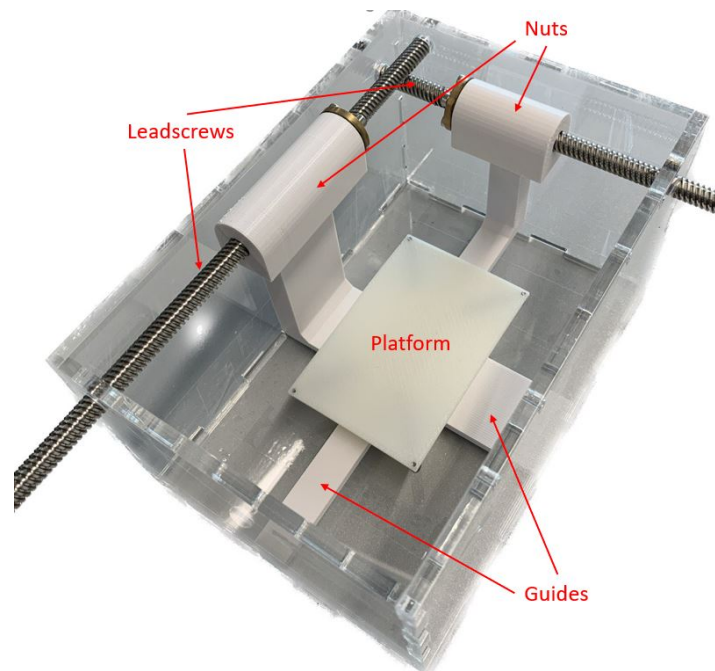


Figure 3.26: The picture shows the first stage of the mechanism and a simplified version of the platform on which the sample will be placed.

The first stage is based on two perpendicular leadscrews that can be actuated from the outside, the rotation of each leadscrew causes the linear motion of one of the two nuts. Every nut is connected directly to the platform through a 90-degree shape guide, hence, the motion of every nut is transferred to the platform (see Figure [3.27](#)). This is possible because the sample holder is placed on a base that has two perpendicular slots to allow the relative movement of the guides. The overall result is a platform able to slide along two different directions independently, just using two external knobs to rotate the leadscrews.

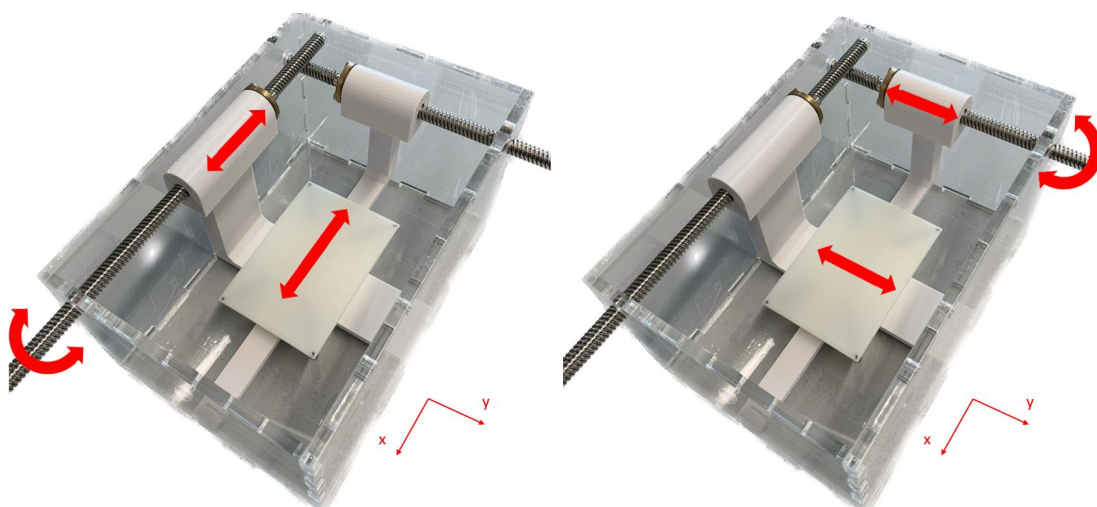


Figure 3.27: On the left, the actuation of the platform along the x-axis. On the right, the actuation of the platform is along the y-axis.



The second stage is meant to implement the two remaining rotational degrees of freedom around the x and y-axis. The mechanism is composed of three gears: two gears ( $g_1, g_2$ ) are fixed to the upper extremities of two leadscrews embedded in the platform. The third gear ( $g_3$ ) is fixed on the top side of the box and can be actuated from the outside. Moreover, like in the first stage, there is a nut around each leadscrew. The idea is to move the platform parallel to the xy-plane through the first stage and couple  $g_3$  to  $g_1$  or  $g_2$ . Once the gears are coupled, it is possible to convert the rotation applied from the outside into linear motion of one of the two nuts, changing the orientation of the sample holder (see Figure 3.28). Once the platform has the desired inclination, the sample can be easily aligned again to the sapphire window through the first stage to be subsequently ablated.

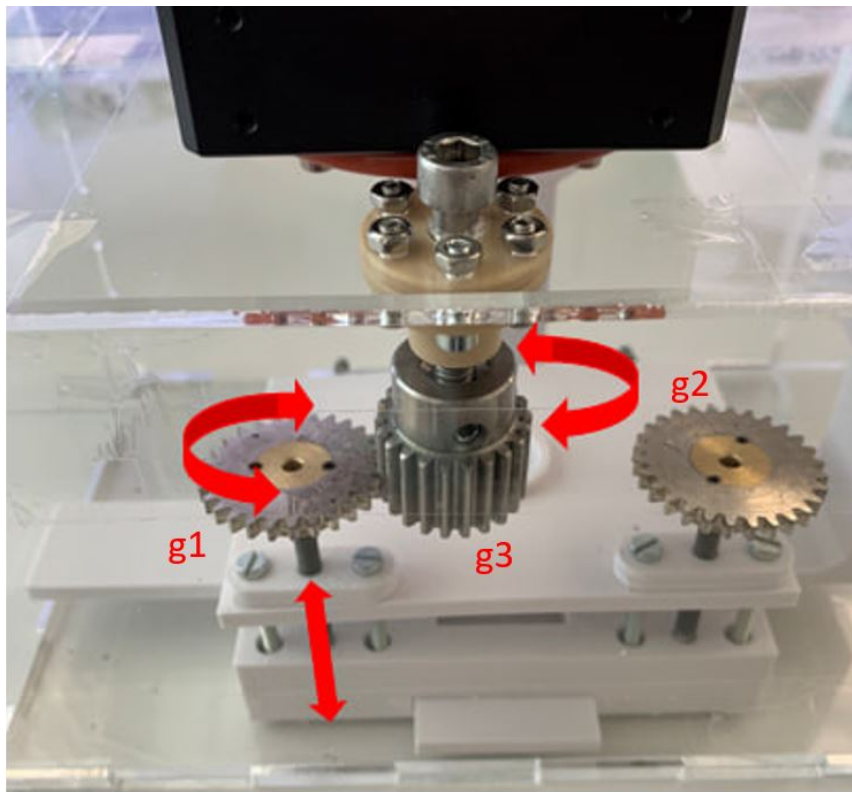


Figure 3.28: The picture shows how the second stage works if the gear  $g_3$  is coupled to the gear  $g_1$ .

The force generated by the two nuts is applied directly to the corners of the sample holder while on the opposite corners, the restoring forces developed by the springs prevent the sample holder from detaching. So, because the forces applied by the nuts cause a variation of the tilt of the sample holder along two independent directions and because of the spherical joint between the sample holder and the base, the stage is able to achieve the two rotational degrees of freedom (see Figure 3.29).

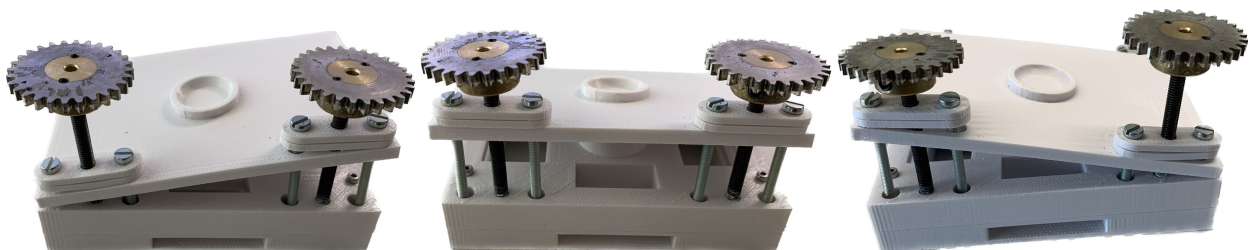


Figure 3.29: Three different possible spatial orientations achievable through the described stage.

The main limitation of the described design is given by the inability to lift up the platform to extract the sample from the nutrition liquid and then submerge it again when the ablation is completed. The available space would not be enough for a more complex inner mechanism. For this reason, a reservoir was added to the design to have a second available compartment where the nutrition liquid can be momentarily transferred during the ablation and then restored inside the main box at the end of the procedure. The reservoir is linked to the box using two tubes to allow the flow of the liquid keeping the pressure equalized. The user has just to move the reservoir above or under the level of the fluid in the box (see Figure [3.30](#)).

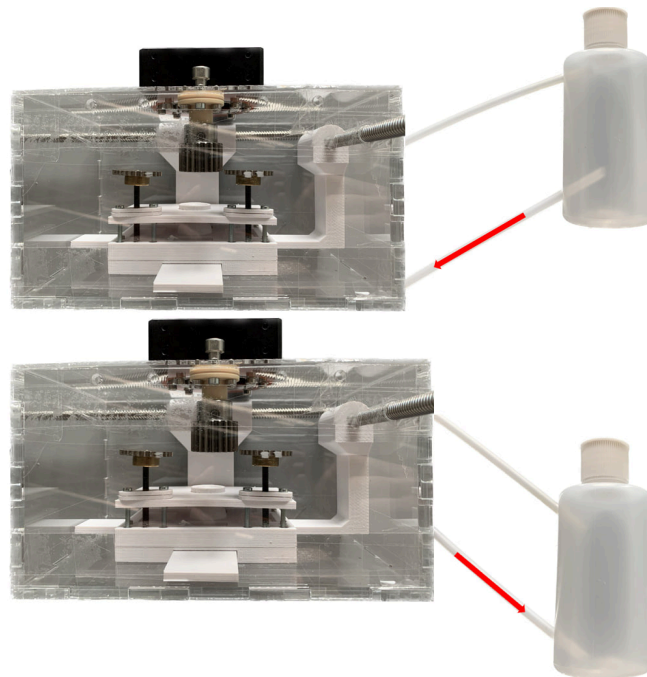


Figure 3.30: In the picture the two possible configurations: when the reservoir is above the level of the fluid in the box, the fluid flows towards the box and vice versa when it is under.

### 3.7.2 Pros and cons

As for the first prototype, the main focus of this analysis is to evaluate the overall usability of the device and underline possible drawbacks before manufacturing.

- **Biocompatibility:** Again, like in the previous prototype, the inner mechanism and the platform are made of 3D-printed material, while the outer box is built using acrylic plastic. Hence, the prototype is not suitable for applications where biocompatibility is one of the main requirements. On the contrary, the external reservoir and the tubes could be successfully used being manufactured in polypropylene.
- **Sterility:** Also in this case, silicon rings are necessary to guarantee water and air tightness in the proximity of the holes drilled to insert the leadscrews and to attach the sapphire lid. Assuring water tightness may be more challenging around the insertion points of the tube used to link the box and the reservoir, in fact, the fluid would constantly submerge them and this may lead to some leaks. Of course, the prototype cannot still be autoclaved.
- **Laser transparency:** The two translational degrees of freedom implemented by the first stage allow the user to move the platform with a quite wide range of motion, in this way, every portion of the sample can be aligned with the laser source and the sapphire window. Furthermore, the external reservoir solves the energy dissipation issue due to the shielding effect of the nutrition fluid. Finally, the distance between the sample and the sapphire glass is about 8 cm (see Figure [3.31](#)), meaning that debris deposit will not be an issue.



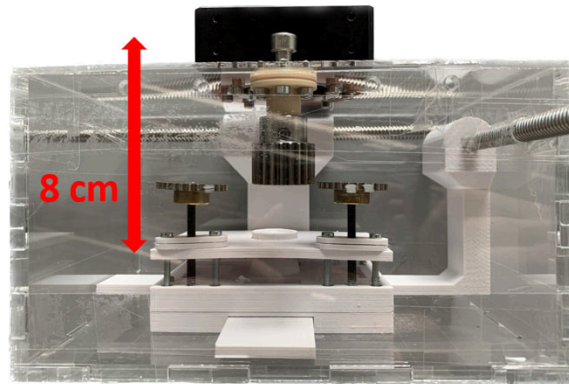


Figure 3.31: The picture shows the distance between the platform and the sapphire glass. The minimum safety distance to avoid debris deposit is about 5 cm.

- **Ergonomy:** The device is able to achieve the four degrees of freedom needed and the platform provides enough space to position the whole tibial plateau. However, the overall ergonomy is limited by the design of the two inner stages. The necessity to couple two gears to change the inclination of the platform makes the positioning process time-consuming. The silver lining is that the positioning stages are highly precise and stable being based on the motion of nuts along leadscrews, the uncertainty is low and related to the thread of the screws. A solution to fix the sample to the platform has still to be figured out.
- **Adaptability:** the prototype allows to ablate the whole tibial plateau at different points which is the most important requirement in terms of adaptability, in this way, it is possible to perform different cuts using different parameters on the same sample. Also, the new overall size and weight of the main box are perfectly feasible with the experimental setup and the only issue will be finding a way to hold still the external reservoir to avoid liquid motion.
- **User-friendliness:** the assembling procedure of the first stage is extremely simple and quick. Instead, the procedure for the second stage is less intuitive and may require some extra time, this may not be a problem if the device is rarely disassembled. However, the platform is aimed to stay constantly in contact with the nutrition liquid where there may be some biological debris and, for this reason, it has to be cleaned frequently and carefully.

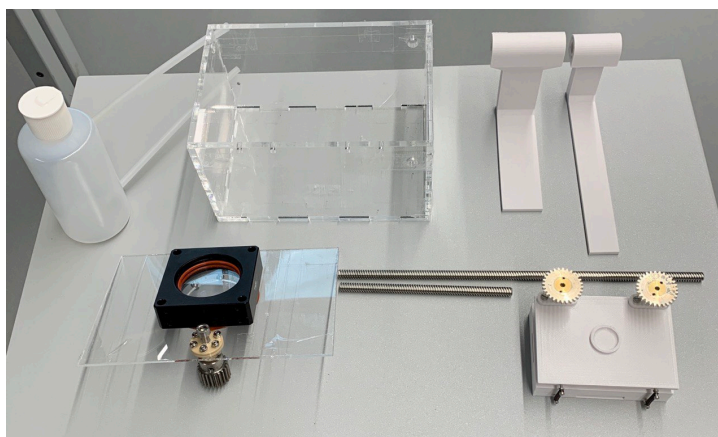


Figure 3.32: The picture shows the second prototype completely disassembled.

From Table [3.6](#) we can see that the model complies with all the requirements related to adaptability, on the contrary, in terms of ergonomy there are some issues caused by the increased level of complexity of the inside mechanism. Besides, compared to the previous prototype, the new one is probably less user-friendly. Sterility and biocompatibility requirements can be completely fulfilled only after the final manufacturing process.

Table 3.6: Requirements with which the second prototype complies (green) or does not comply (red) from the first list.

General requirements	Derived requirements
1. Biocompatibility	Anti-cytotoxic materials Materials suitable for nutrition liquid
2. Sterility	Air-tightness Water-tightness Autoclavable materials Sealable opening
3. Laser transparency	Transparent window for light with a wavelength between 532 and 2940 nm Anti-condensation system Anti-debris design Mechanism to extract the sample from the liquid
4. Ergonomy	Four degrees of freedom sample movement (two translational, two rotational) Easy sample insertion Quick sample positioning Modular design Stable and harmless sample fixation Reproducible positioning At least 8x5 cm space for tibial plateau
5. Adaptability	Entire tibial plateau available Rectangular bottom Max dimensions 15x18x18 cm Max overall weight of the container 5 kg Platform able to support 50 g heavy sample
6. User-friendliness	Highly intuitive assembling procedure Visible inside mechanism Drop robustness

### 3.8 Third list of requirements

The second prototype was ready three months after the beginning of the project, then, the pros and the cons of the new design were closely discussed. Even if it complied with most of the requirements defined after the analysis of the first prototype, it was decided that a third prototype was necessary. The main issue with the second design was that it did not allow a change in the spatial orientation of the sample until the gears were coupled. It means that if the users want to perform two ablations at the same point with two different orientations, they have to take a pause and change the position of the platform in the xy-plane to properly couple the needed gears. This approach basically does not permit adjustment of the orientation of tissue while the OCT scanning is performed. So, because of this and the time-consuming cleaning process, a new prototype had to be developed. Table 3.8 shows how the requirements changed.

Table 3.7: Third list of requirements, the requirements that have been changed compared to the second list are written in blue.

General requirements	Derived requirements
1. Biocompatibility	Anti-cytotoxic materials Materials suitable for nutrition liquid
2. Sterility	Air-tightness Water-tightness Autoclavable materials Sealable opening
3. Laser transparency	Transparent window for light with a wavelength between 532 and 2940 nm Anti-condensation system Anti-debris design Mechanism to extract the sample from the liquid
4. Ergonomy	Four degrees of freedom sample movement(two translational, two rotational) Easy sample insertion Quick sample positioning Modular design Stable and harmless sample fixation Reproducible positioning At least 8x5 cm space for tibial plateau
5. Adaptability	Entire tibial plateau available Rectangular bottom Max dimensions 15x18x18 cm Max overall weight of the container 5 kg Platform able to support 50 g heavy sample Changing the orientation of the sample without changing its position
6. User-friendliness	Highly intuitive assembling procedure Visible inside mechanism Drop robustness Easy and quick cleaning

## 3.9 Third prototype

The third prototype was built through the same techniques used for the other two (laser cutting and 3D printing). The new design is aimed to solve the main issue of the second prototype, which was the necessity of moving the sample from its original position to change its inclination. So, the challenge was to find a solution to solve this problem while keeping all the previous requirements fulfilled.

### 3.9.1 Designing and prototyping

Every component of the prototype was designed again through Solidworks or bought and then assembled to create the device in Figure 3.33. It is composed of two main parts: the box that will contain the sample and the upper part made of an elastic membrane attached to the sapphire window.

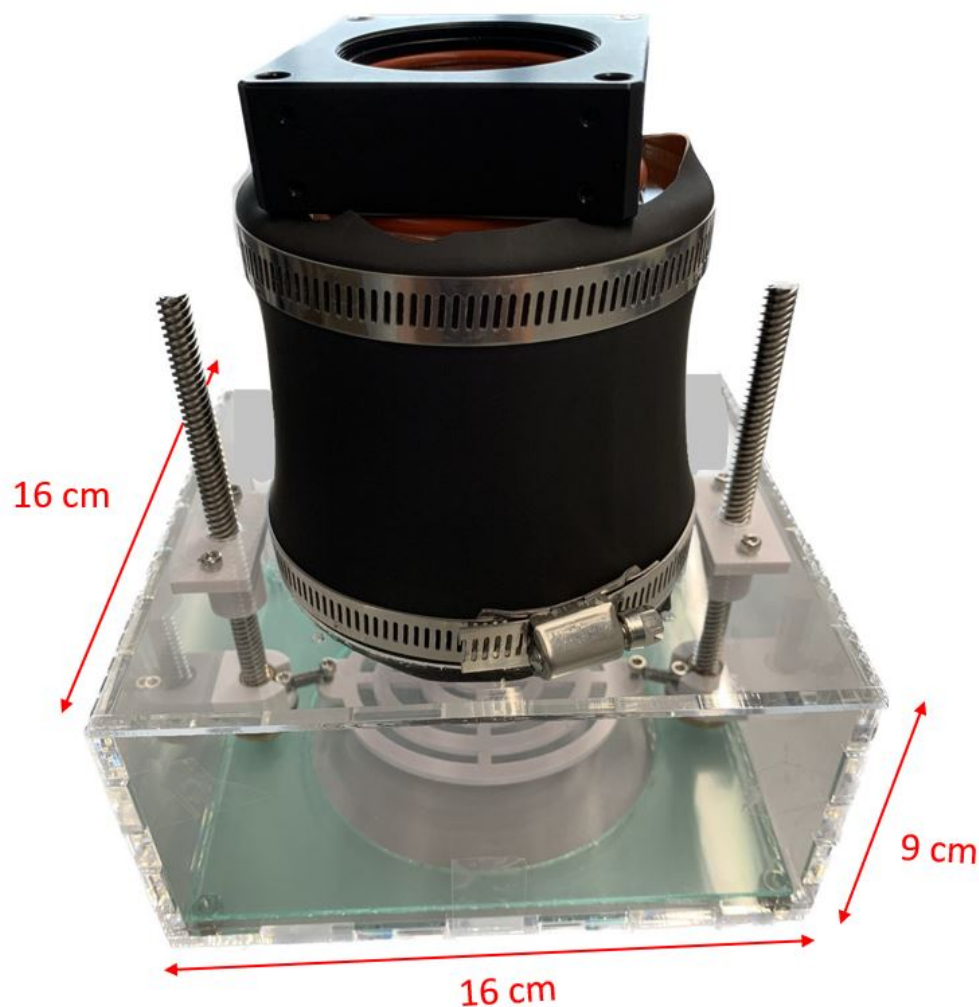


Figure 3.33: The picture shows the third prototype. The dimensions of the box are approximately 9x16x16 cm while the upper part has a diameter of 10 cm

As previously discussed, the device should allow the user to translate the platform along the z-axis to extract the sample from the nutrition fluid. Then, there should be a relative motion between the sapphire window and the platform to ablate different parts of the sample. Finally, the rotations along the x and y-axis are meant to change the tilt of the specimen with respect to the laser beam. To understand how the prototype works it may be useful to first describe separately the two different components. The lower part is composed of three stainless steel leadscrews embedded in a square acrylic box. The leadscrews are meant to change the orientation of the inside platform on which the sample will be placed, this is possible thanks to the three nuts that can slide along the leadscrews. Then the nuts are linked to the platform through three springs (see Figure 3.34).

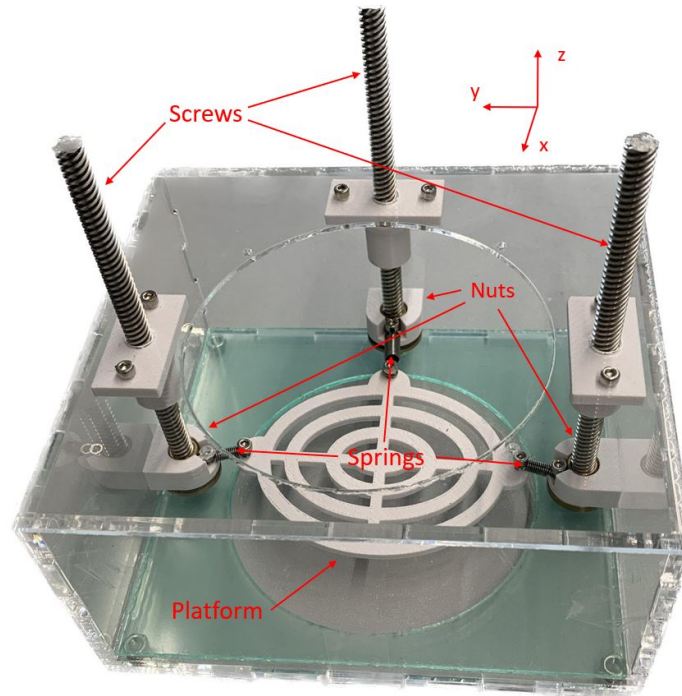


Figure 3.34: The picture shows the main box and the inner mechanism.

The mechanism is designed to extract the sample from the nutrition liquid and then change its orientation through rotations around the  $x$  and  $y$ -axis. If all the nuts are rotated simultaneously, then the platform will move up or down depending on the direction of the rotation (see Figure 3.35). Otherwise, it is possible to achieve different inclinations by rotating just one of the leadscrews. The springs are used as a linker between the nuts and the platform to compensate for the distance changes between the nuts, rigid components would not allow the movement of the platform. The springs keep the sample stable thanks to the restoring forces generated when they are stretched. Besides, springs work as shock absorbers, which may be useful when the device is moved to protect the sample.

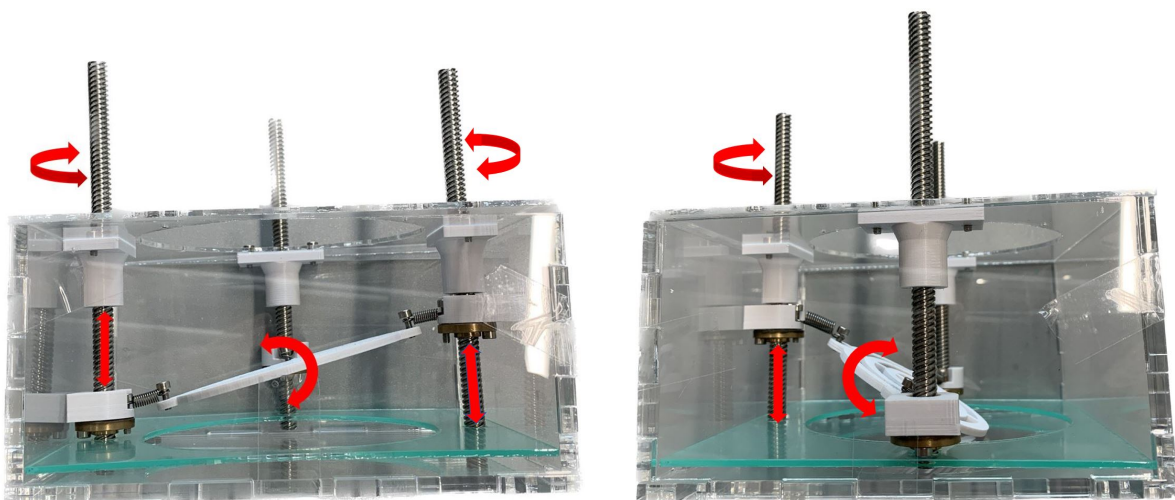


Figure 3.35: On the left the rotation around the  $x$ -axis, on the right the rotation around the  $y$ -axis.

The main issue of this mechanism is the tendency of the leadscrews to be bent by the restoring force of the springs. Two solutions were implemented to solve the problem: a T shape guide attached to the top of the box is placed around each leadscrew and an acrylic layer with three holes for the tips of the leadscrews is positioned at the bottom. In this way, each leadscrew is bound to two different constraints and cannot be bent.



However, using the mechanism previously described and fixing the sapphire window on the top side of the box would not be enough for our purpose. The diameter of the laser transparent glass is around 4.5 cm while the sample can reach 8 cm of length along the ML direction. In this case, the laser could not reach every portion of the tibial plateau. So, it was decided to connect the sapphire window to the rest of the device through a deformable latex membrane able to resist high temperatures and two stainless steel clamps (see Figure 3.36).



Figure 3.36: On the left the two clamps are concentric, on the right they are displaced.

In this way, the two remaining translational DoFs can be implemented from the outside through a two-DoF moving stage. The cage plate containing the sapphire glass can be attached directly to the laser optics and the bottom side of the box to the moving stage. Then, thanks to the deformable membrane, the relative motion between the two fixed points will allow the laser to ablate every portion of the sample (see Figure 3.37). Hence the device is able to achieve 5 DoFs between the platform and the sapphire window.

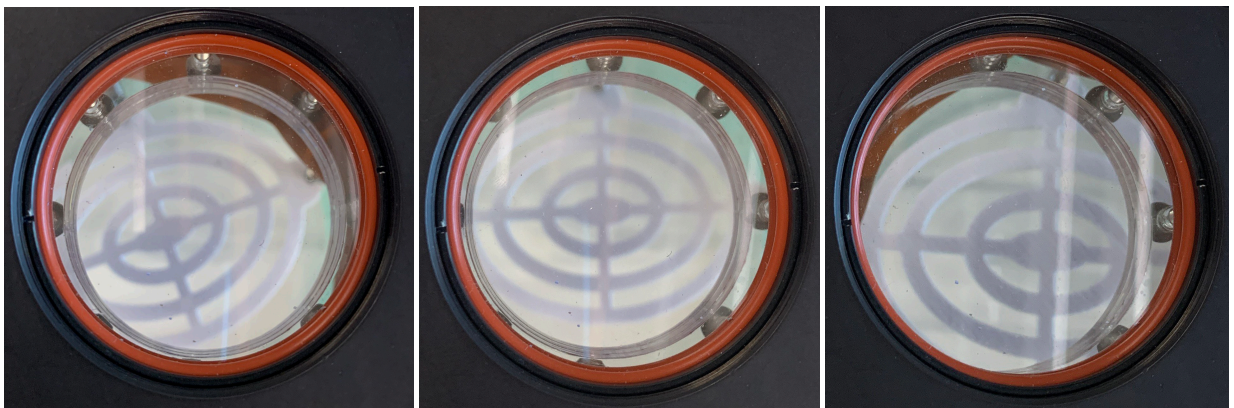


Figure 3.37: The pictures show how every extremity of the platform can be reached by the laser beam by moving the sapphire window relative to the container.

### 3.9.2 Pros and cons

As for the first and second prototypes, the aim of this section is to analyze the easiness of use of the device and detect eventual issues before manufacturing.

- **Biocompatibility:** The situation is the same as the other two prototypes with regard to the box and the inner mechanism. The upper part instead could already be autoclaved, being a combination of a latex membrane, the usual sapphire glass, stainless steel screws and clamps.
- **Sterility:** To assure water and airtightness, three silicon rings have to be used to avoid any leak from the leadscrews holes. Anyway, in this scenario, none of the holes will be constantly submerged by the nutrition liquid. The sealing at the insertion points of the membrane is assured by two adjustable stainless steel clamps (see Figure 3.38). The entire prototype cannot still be autoclaved while the upper part could be, thanks to the high-temperature resistant material.

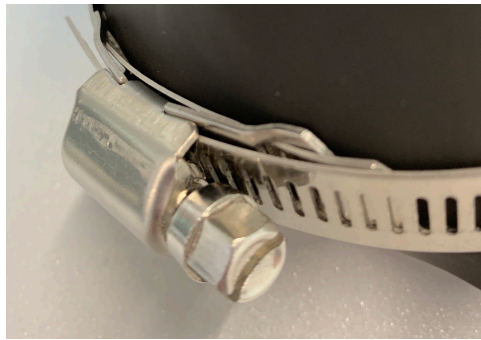


Figure 3.38: The clamps can be adjusted through the screw shown in the picture, ensuring a tight sealing between the membrane and the container.

- **Laser transparency:** The flexibility of the latex membrane solves the issue related to the alignment between the sample and the laser. Besides, the sample can easily be extracted from the liquid thanks to the additional translational DoF along the z-axis given by the simultaneous rotation of the three leadscrews (see Figure 3.39). Again, like in the second prototype, the distance between the sample and the sapphire glass should be enough to avoid debris deposit.

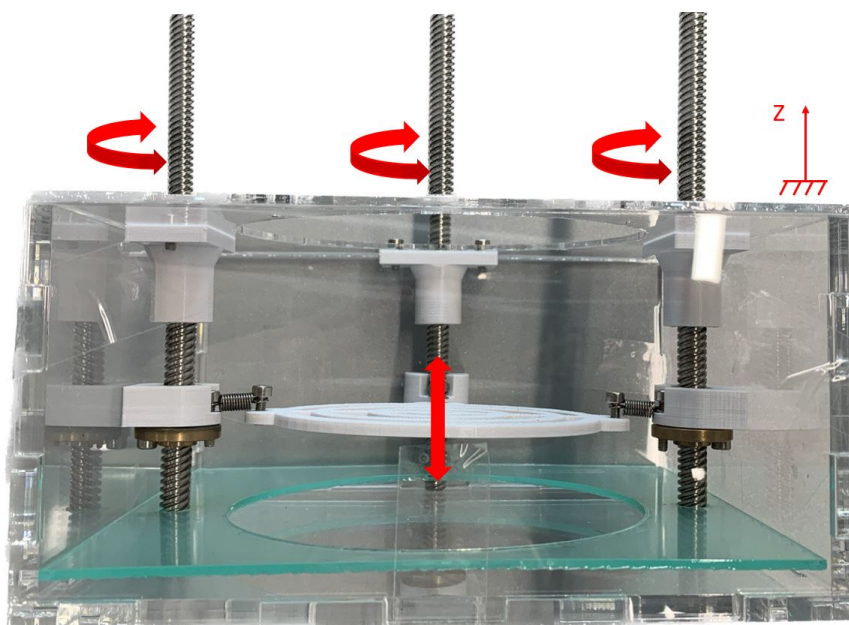


Figure 3.39: The picture shows how the platform can be lifted up and down depending on whether the sample has to be ablated or kept safe and hydrated.



- **Ergonomy:** The device achieves two rotational DoF through the three external knobs. Thanks to the leadscrews, the accuracy and reproducibility of this stage are quite high. However, the main improvement regards how the two translational DoFs are implemented. The sapphire window can just be centered on the sample deforming the membrane. The positioning becomes easy and quick and requires no other complex mechanism. Moreover, the possibility of lifting up and down the sample using the same mechanism makes the design extremely compact.
- **Adaptability:** The new design solves the main issue related to the previous prototype which was the inability to change the tilting of the platform without changing its original position. In other words, every DoF can be actuated independently of each other. Once the laser is aligned with the portion of the sample that has to be ablated, the orientation can be varied anytime. In this case, performing OCT scans during the ablation and, subsequently, fine-tuning the sample orientation will not be anymore a problem.
- **User-friendliness:** The overall assembling procedure is quite easy and quick, the box has just to be closed keeping attention to the correct inserting of the leadscrews in the slots at the bottom. Besides, the cleaning time is highly decreased thanks to the less cumbersome platform.



Figure 3.40: The picture shows the platform used in the third prototype.

Finally, the third prototype was deemed suitable for the final purpose and ready to be manufactured. From Table 3.8 we can see that it complies with most part of the requirements and it solved all the issues pointed out in the old prototypes. The aim of the following phase of manufacturing was to build the prototype using proper materials and fulfill the remaining requirements that rely on the properties of the materials.

Table 3.8: Requirements with which the third prototype complies (green) or does not comply (red) from the first list.

General requirements	Derived requirements
1. Biocompatibility	<p>Anti-cytotoxic materials</p> <p>Materials suitable for nutrition liquid</p>
2. Sterility	<p>Air-tightness</p> <p>Water-tightness</p> <p>Autoclavable materials</p> <p>Sealable opening</p>
3. Laser transparency	<p>Transparent window for light with a wavelength between 532 and 2940 nm</p> <p>Anti-condensation system</p> <p>Anti-debris design</p> <p>Mechanism to extract the sample from the liquid</p>
4. Ergonomy	<p>Four degrees of freedom sample movement (two translational, two rotational)</p> <p>Easy sample insertion</p> <p>Quick sample positioning</p> <p>Modular design</p> <p>Stable and harmless sample fixation</p> <p>Reproducible positioning</p> <p>At least 8x5 cm space for tibial plateau</p>
5. Adaptability	<p>Entire tibial plateau available</p> <p>Rectangular bottom</p> <p>Max dimensions 15x18x18 cm</p> <p>Max overall weight of the container 5 kg</p> <p>Platform able to support 50 g heavy sample</p> <p>Changing the orientation of the sample without changing its position</p>
6. User-friendliness	<p>Highly intuitive assembling procedure</p> <p>Visible inside mechanism</p> <p>Drop robustness</p> <p>Easy and quick cleaning</p>

### 3.10 Manufacturing

This section is where the last version of the developed device is finally presented. The device was entirely realized using autoclavable materials. It is important to observe that not every material is biocompatible, in fact, only the parts that will be continuously in contact with the sample or the nutrition bath need to be so. In the Figure [3.41](#) it is possible to see the final product.

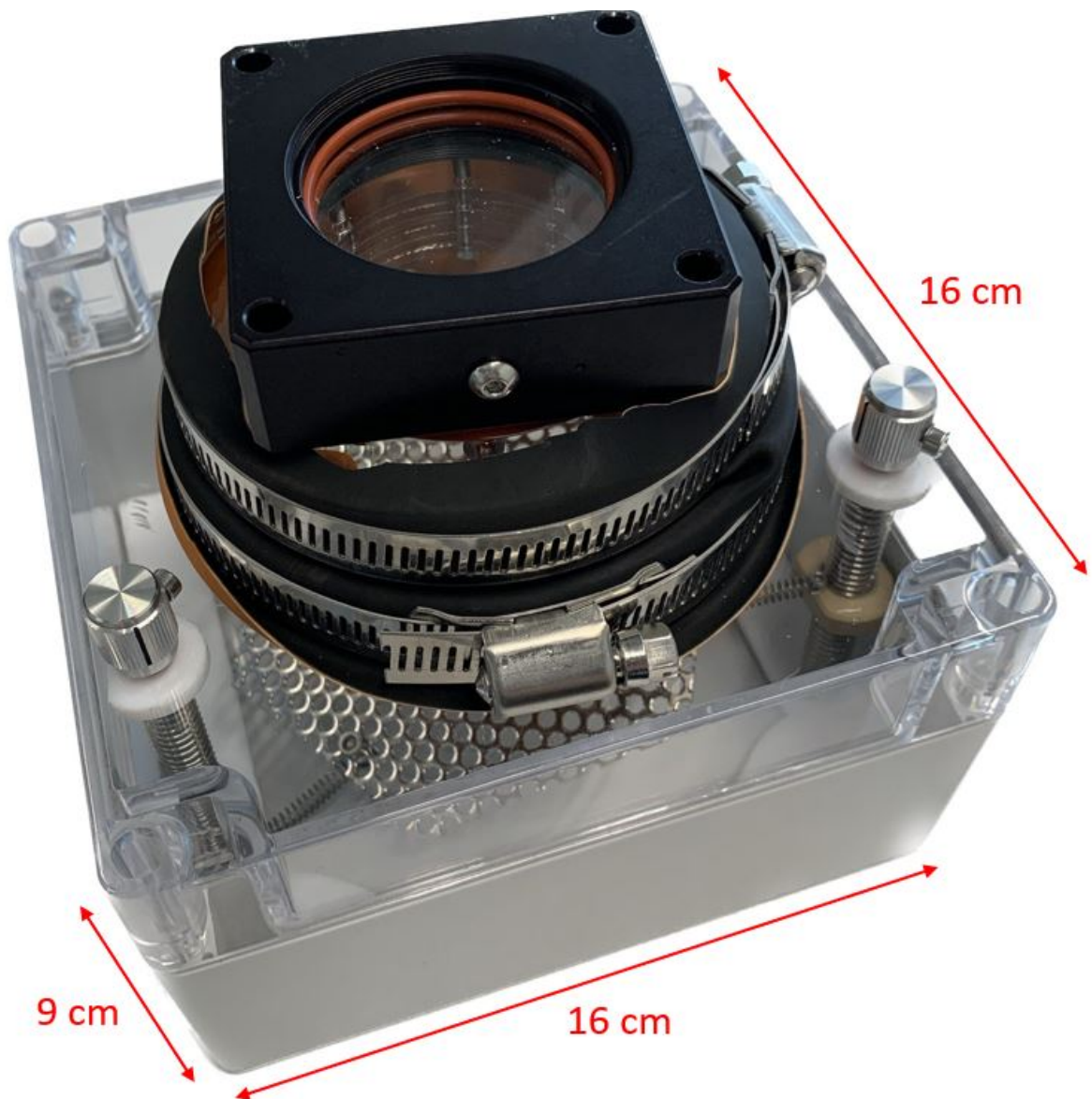


Figure 3.41: The picture shows the final device, the dimensions of the lower box are 9x16x16 cm.

The upper part is exactly the same as that was described in the previous section when the design of the third prototype was discussed. As already said, it is composed of the metallic cage plate that holds the sapphire window, a latex membrane and two stainless steel adjustable clamps. All the parts are autoclavable and biocompatible, except for the latex membrane and the cage plate which are harmful to biological specimens. However, they will not be in contact with the sample or with the fluid as long as the container is not turned upside down. The core of the manufacturing phase was to build the lower box, reducing friction between the moving parts and assuring airtightness.

The starting point was buying a biocompatible box (Figure 3.42) that could fit inside the experimental setup. The box is made of polycarbonate IP65 (RND Components, Nanikon, Switzerland) and can be sealed using four screws, one for each corner. The dimensions of the box allow the device to have enough space for the inner platform and to be feasible for the laser setup.



Figure 3.42: The picture shows the polycarbonate box before the manufacturing.

The next step was drilling four holes in the top side of the box: three holes with a diameter of 0.6 cm for the positioning of the screws and one with a diameter of 10 cm under the sapphire window to let pass the laser beam through (Figure 3.43).

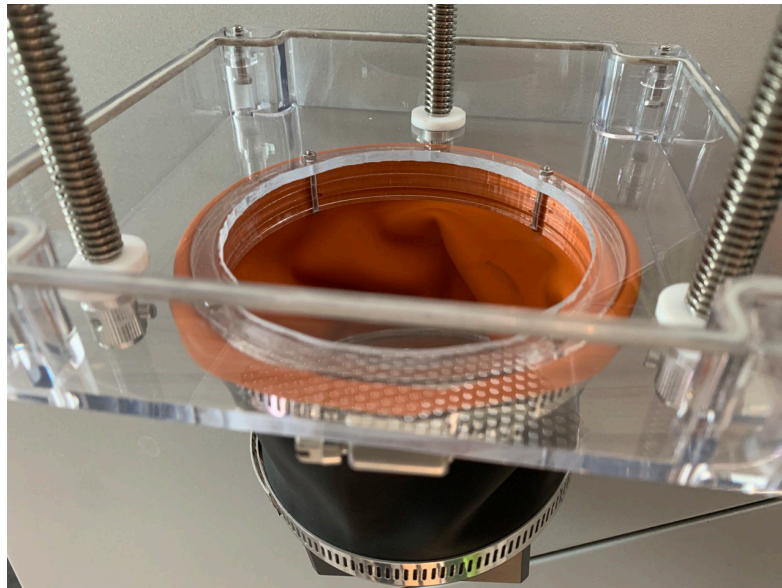


Figure 3.43: The picture shows the four holes drilled in the top side of the box.

After that, it was necessary to replicate the previously described 3 DoF mechanism using suitable materials. The final platform makes use of 3 stainless steel custom-made leadscrews and as many plastic nuts (Igus AG, Cologne, Germany). The thread covers most of the length of the leadscrews except for the extremities that are smooth. In this way, the range of motion of the nut along the screw is quite high and the extremities can be easily fixed to avoid bending issues. The nuts are made of Iglidur J350, a plastic material that can withstand temperatures up to 150 °C (Figure 3.44).





Figure 3.44: The picture shows one of the three custom-made screws and the three nuts. The overall length of the leadscrew is 10 cm.

Then, the nuts are connected through three stainless steel springs to the platform designed to hold the sample. The platform has a hexagonal shape and it was manufactured using a 2 mm thick stainless steel grid (Figure 3.45). The stiffness of the grid is enough to prevent bending due to the forces developed by the springs.

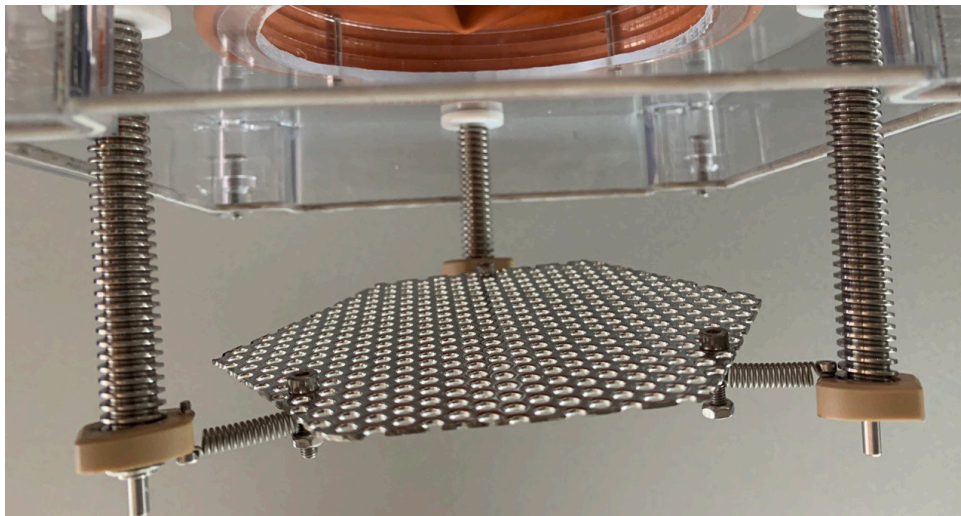


Figure 3.45: The picture shows how the mechanism appears when it is extracted from the box.

The mechanism is actuated from the outside through aluminum knobs (Figure 3.46). Every knob has a cylindrical inner slot with a diameter of 0.6 cm, which is exactly the same diameter as the three smaller holes on the top of the box and as the upper extremity of each screw. In this way, the tip of the leadscrew can pass through the top side and fit inside the knob. Once the knob and the screw are coupled, the lateral set screw embedded in the knob is tightened. Thanks to this coupling, the torque applied to the knob can be transmitted to the corresponding inner leadscrew.



Figure 3.46: The picture shows the top and bottom sides of the aluminum knobs.

However, without further precautions, the coupling would not assure air and water tightness. For this reason, three silicon rings were placed around the protruding extremities of each leadscrew. The pressure between the knob and the polycarbonate box deforms the rings and assures a reliable sealing.

After taking care of the sealing issues, it was time to find a solution to avoid friction between the parts that exhibit a relative motion between them. This aspect was not relevant during the prototyping phase but becomes important when the device is used several times. The risk is that the polycarbonate box may be ruined over time by contact with a material that has a way higher hardness, like stainless steel. This would lead to sealing problems and debris formation inside the container. To prevent that, 3 mm thick Teflon rings were positioned concentrically to the silicon rings but on the other side of the polycarbonate layer (Figure 3.47).



Figure 3.47: On the upper side of the transparent layer, the orange silicon ring. On the other side, the white Teflon ring.

On the other extremity of each leadscrew, the situation is similar. In this case, it was decided to manufacture a square Teflon layer that has the same shape as the bottom of the box and three holes concentric to the screws (Figure 3.48). This component not only solves the issues due to the friction but also prevents the leadscrews from bending.

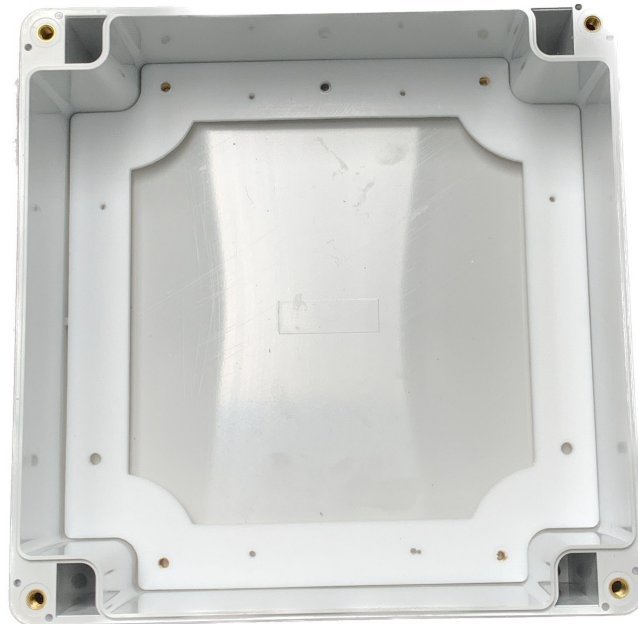


Figure 3.48: The picture shows the bottom of the box and the Teflon component in white.

Moreover, the square Teflon part is quite helpful when the device has to be assembled. In fact, the Teflon layer can be removed from the bottom of the box and positioned around the leadscrews. Then, the upper part can be easily inserted into the lower one (Figure 3.49). At this point, the box is sealed tightening the four corner screws and ready to be used. In Table 3.9, there is a quick recap of the materials used for each part of the final device.

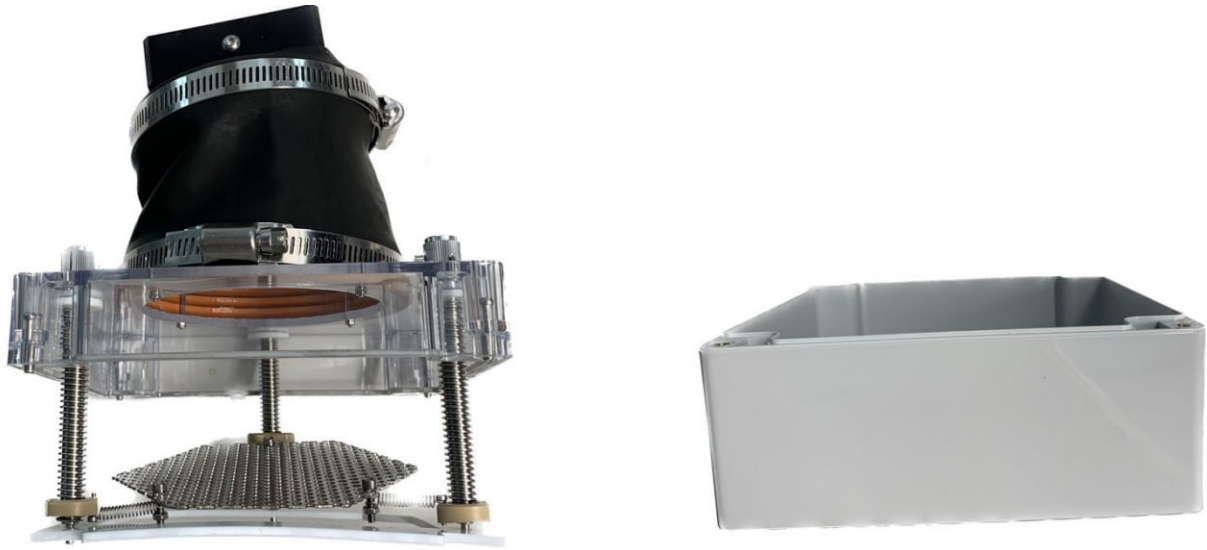


Figure 3.49: The picture shows the bottom of the box and the Teflon component in white.

Table 3.9: List of materials used to manufacture the final device.

Part	Material
Box	Polycarbonate IP65
Springs	Stainless Steel
Knobs	Aluminium
Flexible Membrane	Latex
Cage Plate	Black-Anodized Aluminum
Laser Transparent Window	Sapphire
Sealing Rings	Silicon
Anti-Friction Parts	Teflon
Leadscrews	Stainless Steel
Platform	Stainless Steel
Nuts	Iglidur J350
Clamps	Stainless Steel



## 4 Testing

### 4.1 Sealing tests

The first two tests are meant to evaluate if the device can keep inner sterility once it is sealed. It was decided to test the air-tightness of all the seals and the water-tightness of the seal between the top and the bottom of the box. In fact, the level of the fluid inside the device is not enough to submerge the other seals.

#### 4.1.1 Water-tightness test

The level of the nutrition liquid inside the device is supposed to be enough to cover the sample while it is not ablated. Considering the thickness of the sample 2 cm, the level of the fluid needs to be around 3-4 cm while the distance between the sealing and the bottom is 6 cm (Figure 4.1). So, there would be no need for the sealing to be waterproof if the device is not inclined.

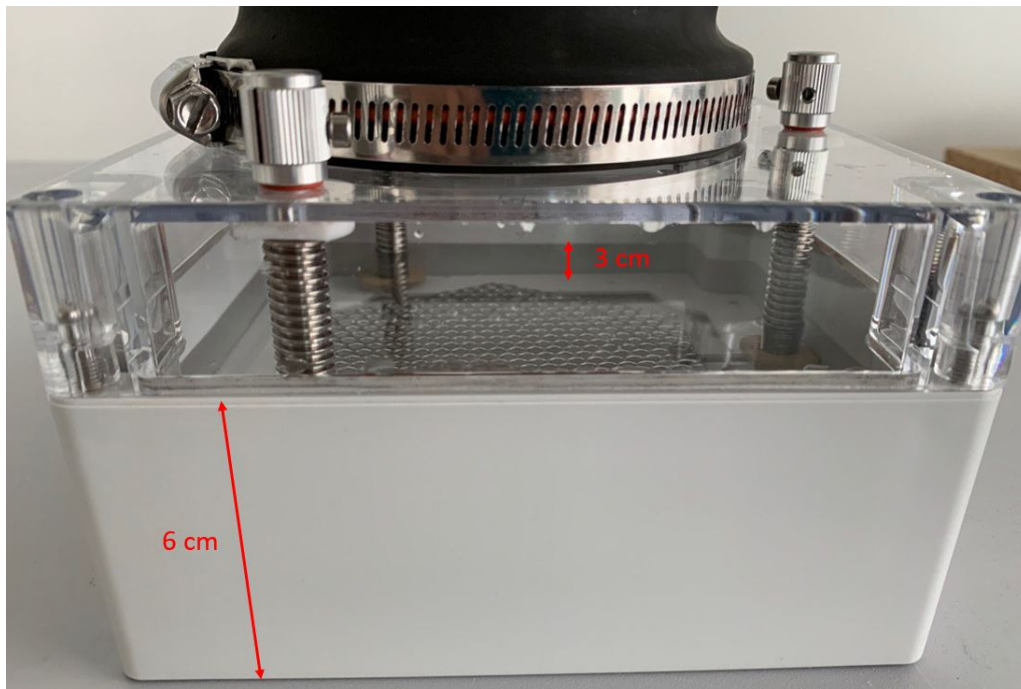


Figure 4.1: Standard-case scenario: the device is filled with water and the height of the fluid is 3 cm, enough to cover completely the platform.

However, the box may be accidentally tilted during transport and some liquid may reach the seal and leak. To ensure that this would not happen, it was decided to test the seal in the worst-case scenario. The device was filled with water until the sealing was completely covered by the fluid (Figure 4.2). Then, it was observed to check if there was any leak.

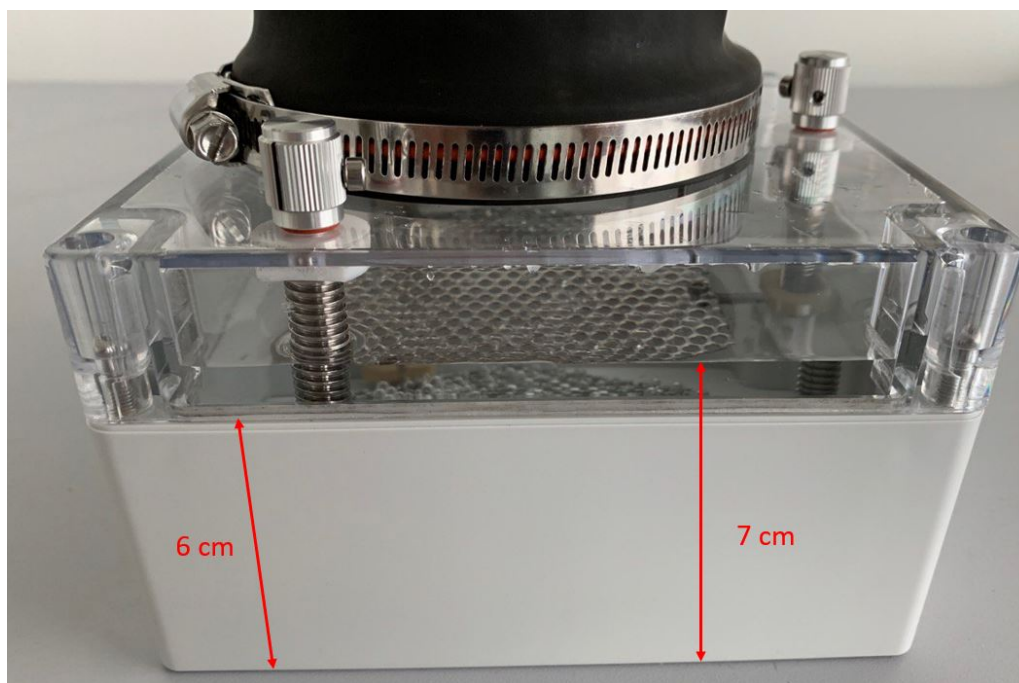


Figure 4.2: Worst-case scenario: the device is filled with water and the height of the fluid is 7 cm, enough to cover completely the seal.

Very soon, some leaks were noticed and it was easy to deduce that the original seal was not water-tight. To solve the problem, a 2 mm thick custom-shape layer of silicon was placed in the junction between the upper and lower part (Figure 4.3).



Figure 4.3: On the left, the upper part of the seal as it was purchased. On the right, the same part after the insertion of the silicon layer .

The test was repeated and, in this case, no leaks were observed in the first minutes. To test the seal in the long term, the height was noted down and compared to the level of water the next day. The two measures perfectly matched, ensuring the water-tightness of the device.

#### 4.1.2 Air-tightness test

The next step was to check if the box was airtight. This aspect is fundamental to avoid any contamination that might alter the outcome of an experiment performed on a sterile sample. After the result of the previous test, it was reasonable to imagine that the main issues may have come from the junctions on the top of the box. In total, there are five seals: three for the knobs and two for the membrane. The holes under the knobs are sealed using silicon rings that are squeezed between the polycarbonate layer and the knobs. Instead, the membrane is attached to the box and the cage plate using two stainless steel clamps (Figure 4.4).



Figure 4.4: On the left, one of the two seals for the membrane. On the right, the seal for the knobs.

After assembling the device, it was immediately clear that there was a problem because the inside air was quickly expelled. In fact, it was possible to pump air in and out by moving the cage plate and deforming the membrane. The airflow was passing through the clamp junctions because the pressure applied from the clamps was not perfectly uniform along the perimeter of the membrane. In particular, it was due to the screw used to adjust the length of the clamp. To uniform the pressure and solve the issue, two silicon rings were placed between the membrane and the clamps (Figure 4.5).

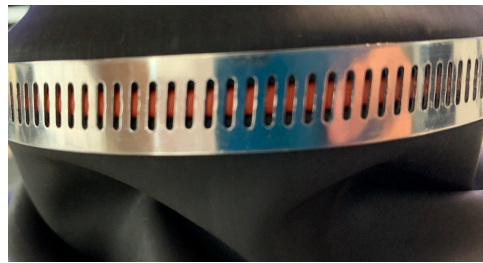


Figure 4.5: The picture shows the silicon ring placed between the membrane and the clamp.

At this point, two tests were performed to see if the device was actually airtight. The box was closed while the membrane was stretched to have more air inside the device, and then the device was left untouched for 4 hours. The height of the cage plate was noted down right after the sealing of the device and checked every hour (Figure 4.6). If there was a leak the weight of the cage plate would have expelled out the air and changed its height.

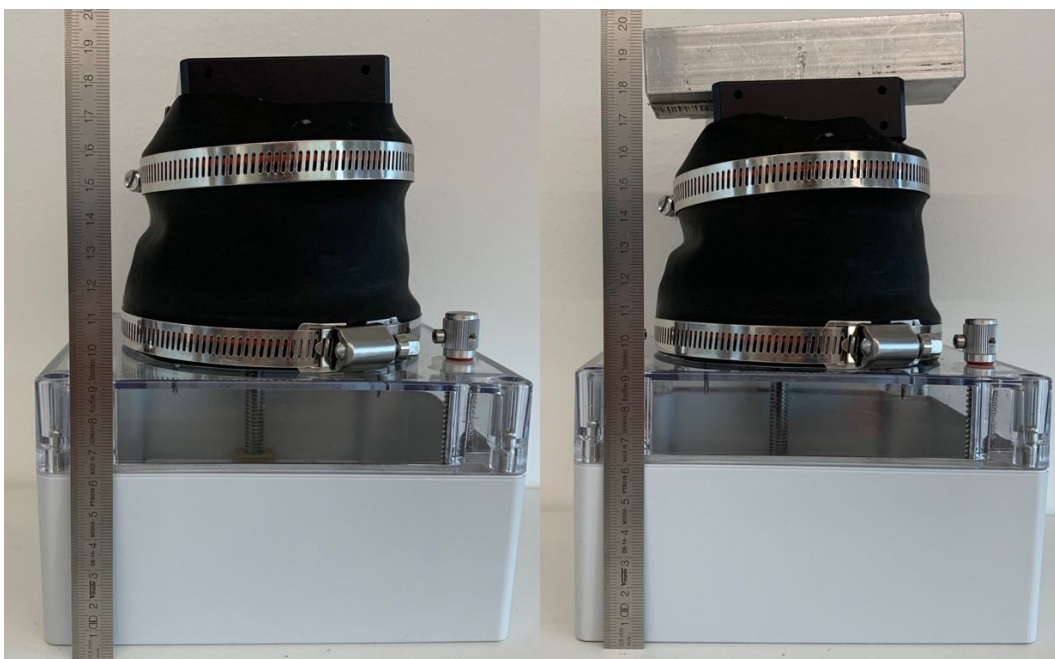


Figure 4.6: On the left, the applied weight to the membrane is 0.2 kg. On the right, it is 0.8 kg.



The height stayed constant despite the pressure due to the 0.2 kg weighing cage plate. The second test was identical to the first one except for the applied weight. In this case, a metallic object was added on top of the cage. The total weight was 0.8 kg, four times more than the weight that is applied in standard conditions. However, the device was able to keep all the air inside, proving its air-tightness.

## 4.2 Usability test

This test is meant to assess if the new container actually improves the overall usability or not. The test consists of performing different procedures using the old device and then the new one in unsterile conditions. In fact, the sample was previously fixed in formalin and the devices were filled with water. In both cases, the sample is fixed to the platform through a stainless steel wire. The aim is to measure the time required for every procedure and detect eventual drawbacks while they are carried out. The evaluated procedures were simply the same procedures that are requested before, during and after a laser experiment: assembling the container, extracting the sample from the fluid, changing the inclination of the platform and disassembling the container. The old device was first analyzed (Figure 4.7) and then it was the turn of the new one (Figure 4.8)

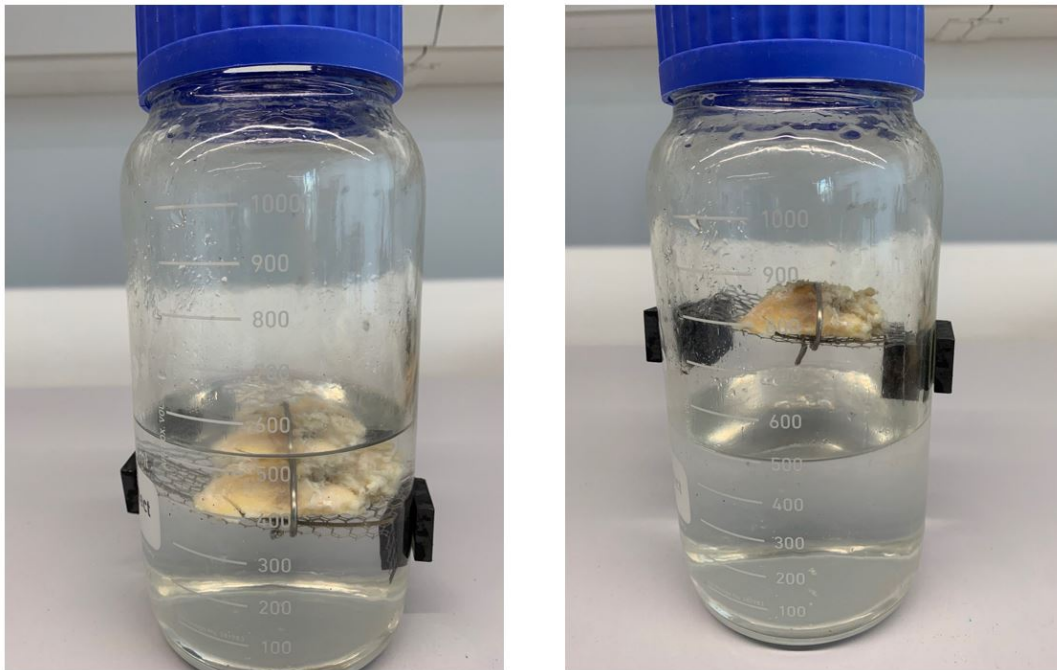


Figure 4.7: The pictures show the sample inside the old container in two possible configurations: submerged and above the level of the fluid.

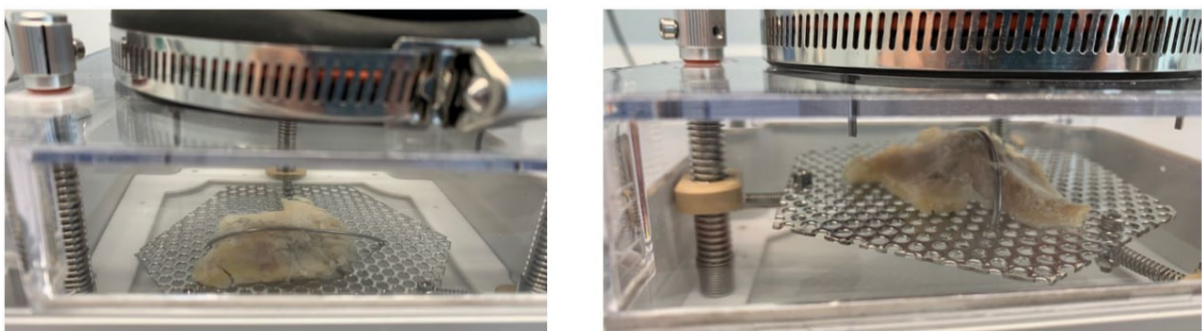


Figure 4.8: The pictures show the sample inside the new container in two possible configurations: submerged and above the level of the fluid.

The results and some considerations are listed below:

- **Device assembling:** The sample has to be placed on the platform and then both have to be inserted in the container, finally the device has to be sealed. For the old model, it took about 2 minutes but it had to be repeated a few times because the sample detached from the platform during the insertion. The new model needs a little more time, around 3 minutes, because the sealing requests to tighten 4 screws. However, it was completed on the first try. In this case, the sample did not detach thanks to the stiffer and wider platform that guarantees a better fixation.
- **Sample extraction:** To perform proper laser ablation, the sample has to be extracted from the fluid. In the old device, it takes about 10 seconds, however, the magnets may detach and let the sample fall down. In the new one, the process needs 1.5 minutes but there is no risk of detaching for the platform.
- **Platform motion:** Changing the inclination of the platform takes a few seconds on both devices. Anyhow, in this case, the needed time is not the most important aspect. Accuracy is what counts when the platform is moved. In the old model, the accuracy cannot be numerically quantified but depends on the user. In the new device, the accuracy of the linear motion of every nut is given by the pitch of the screws that is 1.5 mm. It means that every time the knob makes a full turn, the respective nut translate of 1.5 mm. The use of screws not only ensures high accuracy but also guarantees repeatability in the positioning of the sample.
- **Device disassembling:** At the end of the experiment, the sample has to be recovered to be analyzed. In the old container, it may be uneasy if the sample has comparable dimensions to the diameter of the opening. The new design makes this operation extremely easy once the upper part is separated from the lower one. The requested time is equal to the time necessary to loosen the 4 screws, about 30 seconds.

### 4.3 Autoclave test

The device needs to be sterilized between one experiment and the next one, the easiest way is to autoclave it. The user has just to insert the device in the autoclave (Figure 4.9), select the right sterilization program and wait.

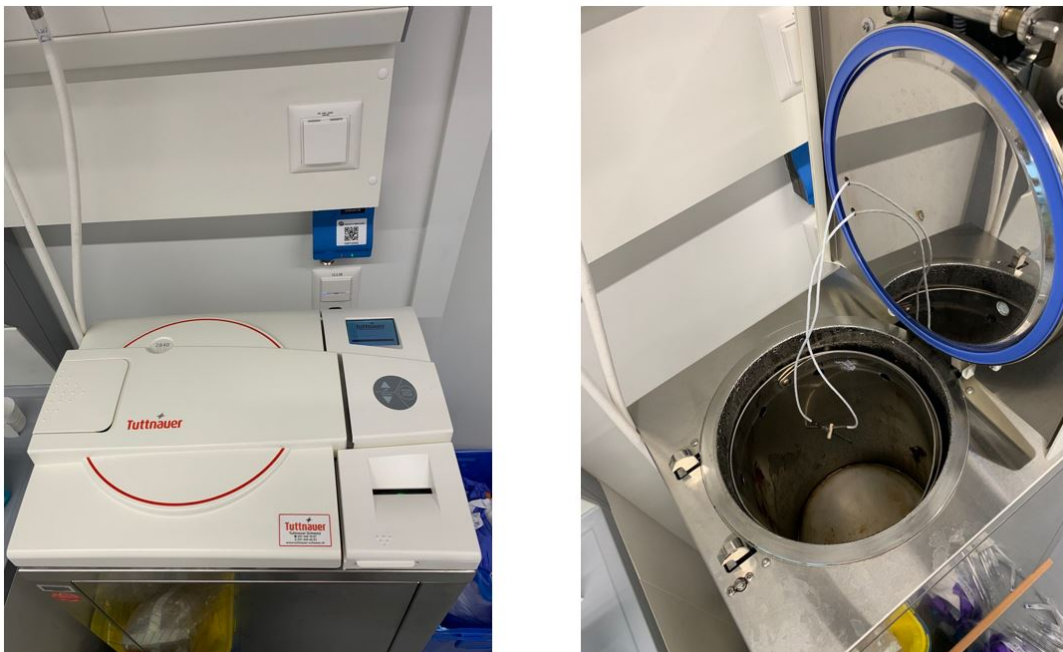


Figure 4.9: Pictures of the autoclave, model "Vertical 3870ELV".

The main drawback of this procedure is that all the materials need to be thermostable up to 121 °C at least. Based on the data sheets of the materials used to manufacture the container, the container should bear temperatures up to 130 °C. However, it was decided to test the device to see if it was actually heat resistant. The autoclave used for the test is a vertical autoclave with an 85-liter internal chamber (Tuttnauer, Bern, Switzerland). The program chosen for the test increases the temperature up to 121 °C, keeps it steady approximately for 15 minutes and then decreases it back to the room temperature. More details in Table [4.1](#)

Table 4.1: Autoclave cycle.

Time (s)	Temperature (°C)	Pressure (KPa)
00:09	22.1	95.9
02:06	21.0	11.5
15:01	70.6	39.7
22:36	99.4	110.5
30:46	121.4	213.3
37:43	121.5	212.6
45:49	121.6	213.2
50:30	101.3	96.3

At the end of the cycle, the device was extracted, assembled and checked. The knobs were the first parts analyzed to understand if the device was deformed during the cycle. It was still possible to rotate them effortlessly, demonstrating that the distance between the different components did not change. Then, the water and air-tightness tests were repeated to see if the silicon rings or the membrane were damaged. Silicon rings did not lose their properties while the membrane seemed stiffer after cooling down. Anyway, the residual elasticity was still enough to move the cage plate all over the platform. So, in conclusion, the container can be autoclaved without serious degradation problems.

#### 4.4 Laser setup fitting test

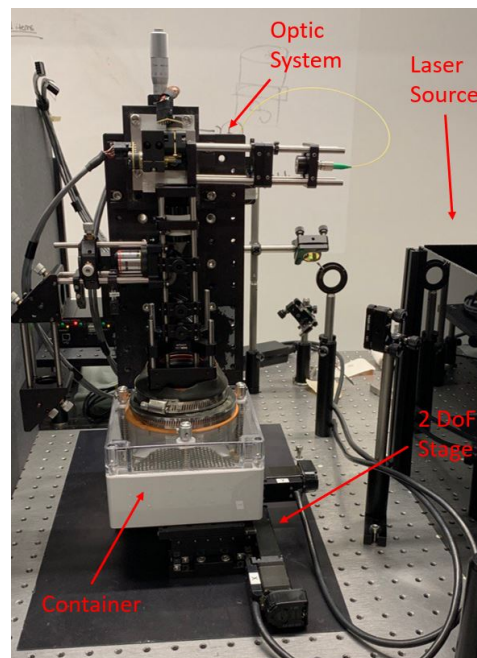


Figure 4.10: Experimental setup.



The last test was done to check if the container could actually fit in the experimental laser setup. The setup is composed of a light source, an optic system, the custom container and a 2 DoF supporting stage (Figure 4.10). Being just a simple feasibility test, the visible green light was used instead of a real laser beam. In this way, it is possible to see if the sample is reached by the laser without risks to the attendants. The optic system is based on lenses and is designed to direct the light from the source to the target place inside the container. The bottom of the container is placed directly on the 2 DoF stage while the sapphire window is attached to the rest of the optic system through some screws (Figure 4.11). Thanks to the flexible membrane, the lower part of the device can follow the movements of the 2 DoF stage while the upper part remains still. In other words, the sample can be moved along the plane perpendicular to the laser beams.

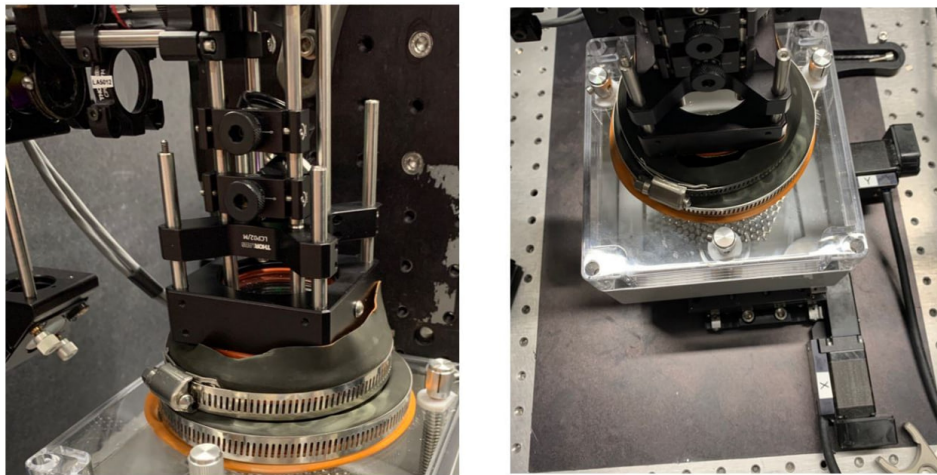


Figure 4.11: On the left, the attachment between the cage plate and optic system. On the right, the 2 DoF stage is placed under the container.

The outcome of the test was positive, the container fitted perfectly in the setup and the green light reached the center of the platform without impediment problems (Figure 4.12). It is still necessary to find a way to firmly attach the bottom of the container to the 2 DoF stage. Besides, the latex membrane may be too stiff to be deformed by the force generated from the motors of the stage.

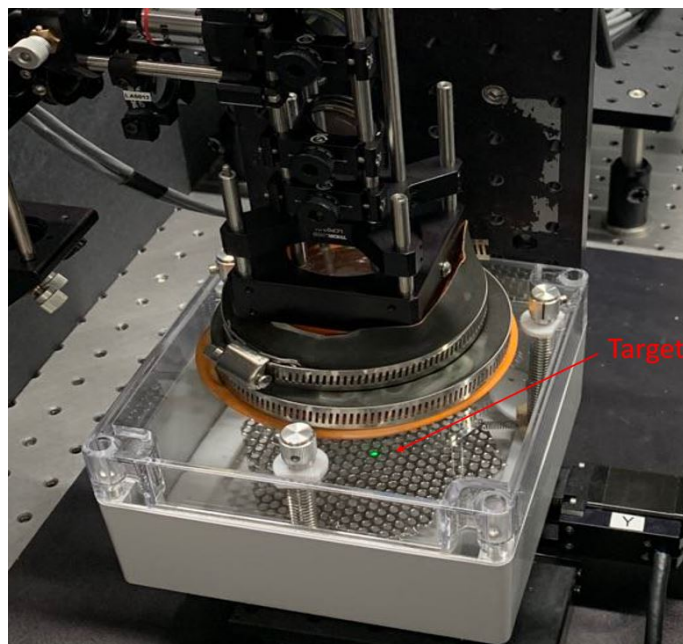


Figure 4.12: The green point shows where the laser beam would perform the ablation.



## 5 Conclusion

### 5.1 Summary

After performing the tests described in the previous chapter, it is finally clear which requirements are fulfilled by the device and which ones are not.

- **Biocompatibility:** Not all the materials used to manufacture the device are considered biocompatible, like latex and aluminum for example. However, if the container is used properly, the sample and the nutrition liquid will make contact with only biocompatible materials. Stainless steel, Polycarbonate IP65 and Iglidur J350 are stable in aqueous solutions and do not release harmful substances.
- **Sterility:** The device can be easily sterilized through autoclave cycles, thanks to the heat-resistant materials it is made of. Then, once it is sealed, it is able to avoid inner contamination as proved by the water and air-tightness tests.
- **Laser transparency:** The new container is based on the same sapphire window used in the previous experiments, it guarantees transparency to the wavelengths of interest (Figure 5.1). Moreover, the innovative design allows the extraction of the sample from the fluid and avoids debris deposits on the window. An integrated solution to prevent condensation is still missing.

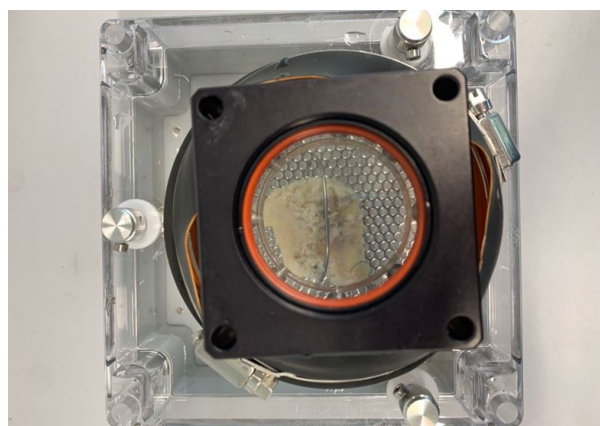


Figure 5.1: A picture from the usability test.

- **Ergonomy:** The main improvements are related to the device's usability in an experimental setup. Attaching the sample to the platform is easy and quick thanks to the modular design and the fixation is stable because of the stiffness of the platform. Besides, the 5 DoF design allows the laser beams to reach the sample at different points and with different angles of incidence. The use of screws makes the positioning repeatable and very accurate.
- **Adaptability:** The final device complies with the requirements in terms of size, shape and weight. Unlike in the previous container, the new inner platform is enough large to hold the entire tibial plateau. Furthermore, the new device is suitable for an experimental setup that makes use of OCT imaging techniques.

- User-friendliness: The assembling procedure is easily understandable, even if the user was not involved in the design process. During the cleaning process, it is important to handle gently the screws to not stress excessively the polycarbonate layer between each screw and the respective knob. Drop robustness is not guaranteed.

The requirements fulfilled by the final device are shown in Table [5.1](#)

Table 5.1: Requirements with which the final device complies (green) or does not comply (red) from the third list.

General requirements	Derived requirements
1. Biocompatibility	Anti-cytotoxic materials Materials suitable for nutrition liquid
2. Sterility	Air-tightness Water-tightness Autoclavable materials Sealable opening
3. Laser transparency	Transparent window for light with a wavelength between 532 and 2940 nm Anti-condensation system Anti-debris design Mechanism to extract the sample from the liquid
4. Ergonomy	Four degrees of freedom sample movement (two translational, two rotational) Easy sample insertion Quick sample positioning Modular design Stable and harmless sample fixation Reproducible positioning At least 8x5 cm space for tibial plateau
5. Adaptability	Entire tibial plateau available Rectangular bottom Max dimensions 15x18x18 cm Max overall weight of the container 5 kg Platform able to support 50 g heavy sample Changing the orientation of the sample without changing its position
6. User-friendliness	Highly intuitive assembling procedure Visible inside mechanism Drop robustness Easy and quick cleaning

## 5.2 Conclusion

A custom workflow to preserve the sterility of the sample was already designed and validated using the old container. It describes the different steps that have to be followed to avoid contamination, from the harvesting during surgery until the final survey (Figure 5.2). After the sample is collected, it is transferred to the container that was previously sterilized through an autoclave cycle. At this point, the sample can be transported anywhere without risk of contamination. Once the experiments are completed, the sample is extracted from the container and analyzed in a proper sterile environment.

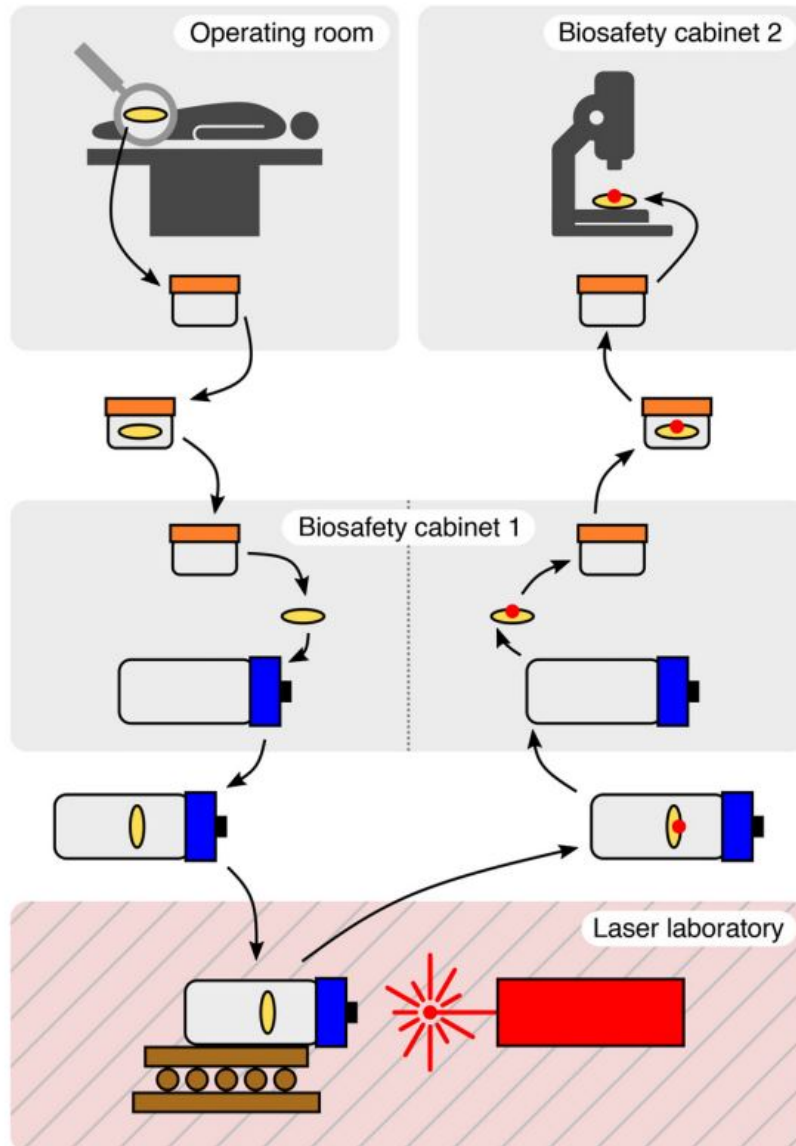


Figure 5.2: Workflow, from the harvesting of the sample to the post-experiment analysis [4].

The new device will be integrated into the existing workflow, ensuring the mandatory requirements in terms of sterility and biocompatibility but providing better usability. The quality of the experiments should benefit from the improvements brought by this project, leading to more reliable outcomes. The next step will be using this device to further investigate laser-cartilage interactions first in an ex vivo laboratory setting, and eventually in vivo trials.

### 5.3 Future work

Even if the final device almost fulfills the list of requirements conceived and updated during the project, there still are some aspects that could be improved. Some of them were known since the beginning but were reputed as less important, others, instead, became clear only after the testing process was carried out. The following list is meant to point out the drawbacks of the current design and how may be possible to further improve the overall performance of the device in the future.

- **Anti-condensation system:** Complying with this requirement was not so urgent because there already was a backup solution. The condensation issue was solved through a hot air gun in the previous experiments. The idea was to develop an integrated anti-condensation system that could replace the use of a hot air gun. Unfortunately, after the final assembly, there was not enough time to implement a proper alternative. Having a heating system embedded in the device would probably simplify the experiments, making a second device unnecessary.
- **Knobs:** The knobs currently used are long less than 3 cm, which makes grabbing them a bit uneasy. Buying longer knobs may solve the issue, otherwise, a 3D-printed part may be used to increase the grip.
- **2 DoF stage fixation:** The bottom of the container already has some holes for screws, however, they are not compatible with the holes in the 2 DoF stage. If the container is not firmly attached, the precision of the ablation will be affected. It is necessary to include a third part that has holes for the screws of both the container and the stage.
- **Membrane stiffness:** The rigidity of the latex membrane was not considered relevant until the device was placed in the experimental setup. Probably, the stiffness is too high to allow the relative motion between the 2 DoF stage and the optic system. The force produced from the actuators of the stage may not be enough to deform the membrane. The easiest solution would be to replace the latex with another autoclavable and less stiff material.

# Bibliography

- [1] A. Zam, "Laser-tissue interaction," in *Springer Nature Switzerland AG 2020 25S. Stubinger et al. (eds.), Lasers in Oral and Maxillofacial Surgery*, 2020.
- [2] R. Friedli, "Robot-assisted laser ablation on engineered human cartilage implementation of custom ablation shapes and evaluation of chondrocyte viability," in *Swisscovery UniBas*, 2022.
- [3] Y. Zhang *et al.*, "Comparison between three-dimensional ct and conventional radiography in proximal tibia morphology," in *Wolters Kluwer Health*, 2018.
- [4] C. Duverney *et al.*, "Sterile tissue ablation using laser light—system design, experimental validation, and outlook on clinical applicability," in *Journal of Medical Devices Copyright VC 2021 by ASME MARCH 2021, Vol. 15 / 011104-1*, 2021.
- [5] G. Rauter, "The miracle," in *Springer Nature Switzerland AG 2020 25S, Lasers in Oral and Maxillofacial Surgery*, 2020.
- [6] A. Barbero *et al.*, "Nasal chondrocyte-based engineered autologous cartilage tissue for repair of articular cartilage defects: an observational first-in-human trial," in *Lancet 2016; 388: 1985-94*, 2016.
- [7] J. A. Buckwalter and J. A. Martin, "Osteoarthritis," in *Adv Drug Deliv Rev 2006; 58: 150-67*, 2006.
- [8] A. J. Detterline *et al.*, "Treatment options for articular cartilage defects of the knee," in *Orthop. Nurs. 24(5), 361-366 (2005)*, 2005.
- [9] G. Lehoczky, F. Wolf, M. Mumme, S. Gehmert, S. Miot, M. Haug, M. Jakob, I. Martin, and A. Barbero, "Intra-individual comparison of human nasal chondrocytes and debrided knee chondrocytes: Relevance for engineering autologous cartilage grafts," *Clinical Hemorheology and Microcirculation*, 2020.
- [10] A. Barbero *et al.*, "Engineered nasal cartilage for the repair of osteoarthritic knee cartilage defects," in *SCIENCE TRANSLATIONAL MEDICINE*, 2021.
- [11] S. Rosen *et al.*, "Assessment of tissue damage due to mechanical stresses," in *Int. J. Rob. Res., 26(11-12), pp. 1159-1171.*, 2007.
- [12] A. Zam *et al.*, "Laser in bone surgery," in *Springer Nature Switzerland AG 2020 25S. Stubinger et al. (eds.), Lasers in Oral and Maxillofacial Surgery*, 2020.
- [13] J. D. Richmon *et al.*, "Compressive biomechanical properties of human nasal septal cartilage," in *American Journal of Rhinology*, 2006.
- [14] J. T. Gu and B. J. F. Wong, "Cartilage reshaping," in *Springer Nature Switzerland AG 2020 153S. Stubinger et al. (eds.), Lasers in Oral and Maxillofacial Surgery*, 2020.
- [15] A. Arslan, "Cell damage spreading in manually and laser ablated cartilage samples," in *Swisscovery UniBas*, 2022.